EXPLORING LIFT-OFF DYNAMICS IN A JUMPING ROBOT

A Thesis
Presented to
The Academic Faculty

by

Jeffrey J. Aguilar

In Partial Fulfillment
of the Requirements for the Degree
Master of Science in the
School of Mechanical Engineering

Georgia Institute of Technology
December 2012

EXPLORING LIFT-OFF DYNAMICS IN A JUMPING ROBOT

Approved by:

Professor Harvey Lipkin, Committee Chair
School of Mechanical Engineering
Georgia Institute of Technology

Professor Daniel I. Goldman, Advisor
School of Physics
Georgia Institute of Technology

Professor Alexander Alexeev
School of Mechanical Engineering
Georgia Institute of Technology

Date Approved: 1 July 2010

To my family,

without whose support and guidance, I would not be who I am today.

ACKNOWLEDGEMENTS

I would like to thank my advisor Prof. Daniel Goldman for taking me on as a student and giving me invaluable guidance in these murky waters that are graduate school. He has always pushed me to do my best and has molded me into the researcher I am today. He has given me a graduate school experience that I will cherish for years to come. I would also like to thank my gracious co-advisor, Prof. Harvey Lipkin, who took me on as a student in the Mechanical Engineering department, and has also helped me with support by considering me to become his TA for Robotics ME 4451, which was an invaluable experience. I give thanks also to Prof. Alexander Alexeev for taking the time to be a part of my thesis committee.

I give thanks to Dr. Paul Umbanhowar at Northwestern University for his continued interest in my work as well as helpful discussions in the early stages of my project. Without his insight, I would not have considered using a continuity sensor to detect lift-off.

I am also indebted to an incredible ensemble cast of CRAB Lab members and alumni - Dr. Ryan Maladen, Dr. Yang Ding, Dr. Chen Li, Sarah Sharpe, Nick Gravish, Nicole Mazouchova, Andrei Savu, Feifei Qian, Tingnan Zhang, Mark Kingsbury, Mateo Garcia, Andrew Masse, Robyn Kuckuk and Vlad Levenfeld for making lab life fun and exciting. Special thanks to Andrei Savu for helping me construct my experimental apparatus. Special thanks to Nick Gravish for helping with automation setup. And special thanks to Sarah Sharpe, Nicole Mazouchova, Yang Ding, Chen Li, and Feifei Qian for always being available to help on pretty much anything.

I am also grateful to my always insightful colleagues, Prof. Kurt Wiesenfeld and Alex Lesov, who I collaborated with for the research presented in this thesis. Their

theoretical insight and effort in our project has gone hand in hand with my work and cannot be understated how valuable their input has been. Special thanks go out to Alex for leading the charge in the effort of the theoretical analysis of my experimental results.

I would like to thank my parents for supporting my endeavors and always being there for love and guidance. I would also like to thank my brother, cousins and all of my friends for also supporting me and being there to make the rest of my daily life incredible.

The National GEM Consortium, the Burroughs Wellcome Fund, Army Research Laboratory, and the National Science Foundation supported this work.

TABLE OF CONTENTS

LIST OF TABLES

LIST OF FIGURES

SUMMARY

Terrestrial organisms and robots are tasked with traversing complex environments in ways that conventional wheeled vehicles are unable to accomplish, and do so by effectively deforming the appendages of their bodies. Jumping is a common mode of locomotion for various animals. It is used as a primary mode of locomotion, to reach higher places, for predation, and also as a survival mechanism. With the advent of robots designed with inspiration from nature's excellent jumpers, it is important to understand the fundamental factors and mechanics that optimize jumping performance. Animals often amplify their jumping power with effective use of compliant structures by performing catapult jumps, squat jumps and countermovements. Certain animals utilize a variant of countermovement known as the stutter jump, where the jump is preceded by a small initial hop. Biologically inspired robots have taken a cue from nature to produce hopping gaits, catapults and squat jumps, yet systematic studies of the movement trajectories that maximize jumping performance are relatively scarce.

This thesis presents a systematic study with a robotic jumping template based on a 1D variant of the spring-loaded inverted pendulum (SLIP) model of jumping to uncover the movement strategies for maximum height jumping when a catapult mechanism is unavailable. While more complex models exist that more closely describe animal movement, we chose the simple SLIP model, which as of yet has only been used to describes gaits such as bouncing and running, because it allows us to directly correlate aspects of jumping performance to underlying characteristics of such a system such as system resonance. The robot was a mass-spring arrangement with an actuated mass, which we oscillated sinusoidally. In concert with simulation, we

systematically varied sinusoidal parameters of the command trajectory for robotic mass actuation to uncover which values provided the best jump performance. Our findings agree with a previous model of maximum height jumping which predicted that the countermovement was better than the squat jump. Specifically, a countermovement produced a stutter jump that is optimal at a frequency lower than the natural frequency, f_0, and a squat jump produced a single jump that is comparably optimal but a faster frequency, which requires more internal power. An analysis of the dynamical model revealed how optimal lift-off results from non-resonant transient dynamics.

The following introductory chapter presents an overview of previous work on jumping animals, robots and theoretical models. Chapter II discusses our experimental approach, including an overview of the mathematical jumping model, methods and materials as well as an introduction to the two experiments performed. Chapters III and IV provide a detailed account of the procedure and results of the two experiments examining minimum forcing amplitude and jump height. Chapter V presents a theoretical analysis of these results, and lastly, Chapter VI presents the conclusions and future work.

CHAPTER I

INTRODUCTION

1.1 Motive and Overview

Terrestrial organisms [10][38] as well as robots [72][94][93] run, climb, and jump over diverse terrain to traverse complex environments in ways that conventional wheeled vehicles are unable to accomplish [13], and do so by effectively bending their multi-jointed appendages and bodies. In particular, jumping is a common mode of locomotion for various animals [46][17][99][73][119][1][28] as well as for robots [13][104][98][45]. Jumping is used as a primary mode of locomotion, to reach higher places, and as survival and predatory behavior [77]. And with the advent of robots taking inspiration from nature's excellent jumpers, there is an imperative to understand the fundamental factors and mechanics that optimize jumping performance.

In animals, size and relative morphological scale of jumping appendages greatly affect jumping performance [123][33]. Yet power output from jumps is much greater than the power output animal muscles produce [17][40][19]. This power amplification comes from elastic energy storage [61], and animals leverage this elasticity through a variety of jumping strategies such as catapults [46], squat jumps [119] and countermovements [74]. Certain animals even utilize a variant of countermovement known as the stutter jump [80][48], in which the jump is preceded by a small preparatory hop.

Biologically inspired robots have taken advantage of these different jumping modes such as catapult jumpers [84][13], hoppers [76][111], and bipedal robots that can perform squat jumps [86][85]. Instead of making simple robotic templates to uncover jumping mechanics, researchers have generally taken an engineering approach

to tackle the inherent challenges of building jumping and hopping robots [104] and optimize predefined modes of movement.

This thesis presents a systematic study with a robotic jumping template based on a simple mathematical model of jumping to uncover the movement strategies for maximum height jumping when a catapult mechanism is unavailable. There have been a few mathematical models proposed for maximum height jumping [5][89], both of which predicted that countermovements perform better than squat jumps in general [5] which has been specifically shown in humans [89]. Hopping has generally bee n characterized by the spring loaded inverted pendulum (SLIP) model [97], which is the basis for most hopping robot designs and is a simpler model than those of maximal height jumping. The basis for our robot is a 1D variant of the SLIP model, which has a mass-spring arrangement with an actuated mass, which we actuate sinusoidally. This model allows the linking of performance metrics to underlying parameters of such a system such as resonance by exploring a relatively small sine wave parameter space.

Within this framework, Chapter II presents the experimental approach, Chapters III and IV provide the procedure and results for two experiments conducted examining minimum forcing amplitude and jump height, and Chapters V and VI present the analyses and conclusion. The following three sections of this Chapter provide an overview of the previous work on jumping animals, jumping robots and theoretical jumping models.

1.2 Jumping Performance in Biology

1.2.1 Introduction

Jumping is an important behavior in biology. Humans use various jumping styles in sports. Other animals jump to escape predators and conversely as a predatory behavior [61][77], to reach higher ground, and even as a primary means of locomotion.

As such, many animals have become specialized in jumping. Cats, bushbabies, frogs, kangaroos and a variety of insects are considered to be among the best jumpers.

There has been considerable interest over the years in understanding the mechanisms of jumping that maximize jumping performance in these various animals. What are the factors that play into the excellent jumping performance [50] in animals? At the most basic level, jumping involves a transient burst of motion in which the muscles of an animal's grounded appendages shorten and lengthen, interacting with the bone and connective tissue to generate a force that propels the body away from the ground, generating lift. It has been found that an increase in size, relative muscle mass used for jumping, and relative limb length can all contribute to increased jumping performance [123][33]. Yet, even with these advantages, it has been found in various animals that the overall power output produced in a jump is many times greater than the maximum amount of power that the muscles involved in producing the jump are capable of providing [17][40][19]. The following sections provide an overview of the research found in various animals where various scaling factors contribute to jump performance as well as the universal method contributing to power amplification in jumping.

We note that there are many metrics used in literature to quantify jumping performance. For example, Wilson et. al. considered take-off velocity, jump distance, maximum power, average acceleration, and contact time in studying how jumping performance changed with body mass amongst striped marsh frogs [116]. These metrics scaled differently among different species and groups, and indeed, the jump performance metrics vary amongst different studies. In our research, we only considered 1D vertical jumping. We used jump height as the performance metric, which is directly related to take-off velocity. In many biological studies, the notion of jump "ability" was used, in which, jump height or distance was compared against the animal's body size, [123],[99]. A similar nondimensionalization is made later in our analysis in which

jump height is scaled with forcing amplitude (for one cycle sinusoidal forcing), which may be analogous to leg length.

Figure 1: Various jumping animals: *Felis catus*, *Galago senegalensis*, *Craugastor fitzingeri*, *Homo sapiens*, *Petrogale xanthopus*, and *Pulex irritans*. Michael Jordan photo courtesy of NBA, other images courtesy of Wikipedia.

1.2.2 Effects of Size and Morphology

Organisms that are adept at jumping exist over a large range of sizes, from fleas to kangaroos. However, when considering what factors affect jumping performance, body scaling seems to be a natural point to examine. See Figure 2(a) for a plot of jump heights for animals of different sizes. Animals with overall larger body sizes typically have large muscle mass and longer length to increase lift off acceleration leading

to higher jump height. There have been numerous studies in which this scaling effect has been examined directly within specific animal species. Zug [123], for example, studied the jumping performance of 84 different species of frogs. The amphibians were tested in rectangular arenas in the laboratory and their jump distances were recorded. Within a species, jumping distances increased with body size, characterized by snout-vent length (head to tail). Similar results were found in Wilson's study of striped marsh frogs when comparing differences in mass to various performance metrics, all of which correlated positively with increases in mass [116]. In a study comparing the jump performance of 15 species of *Anolis* lizards, jump distance increased with an increase in snout-vent length. Demes compared the kinematics of 4 species of Malagasy lemurs of varying body mass [36]. Since the animals were observed jumping in their natural habitat, jump height or distance was not a systematic measure that was reported. However, it was observed that acceleration times increased with increases in body mass.

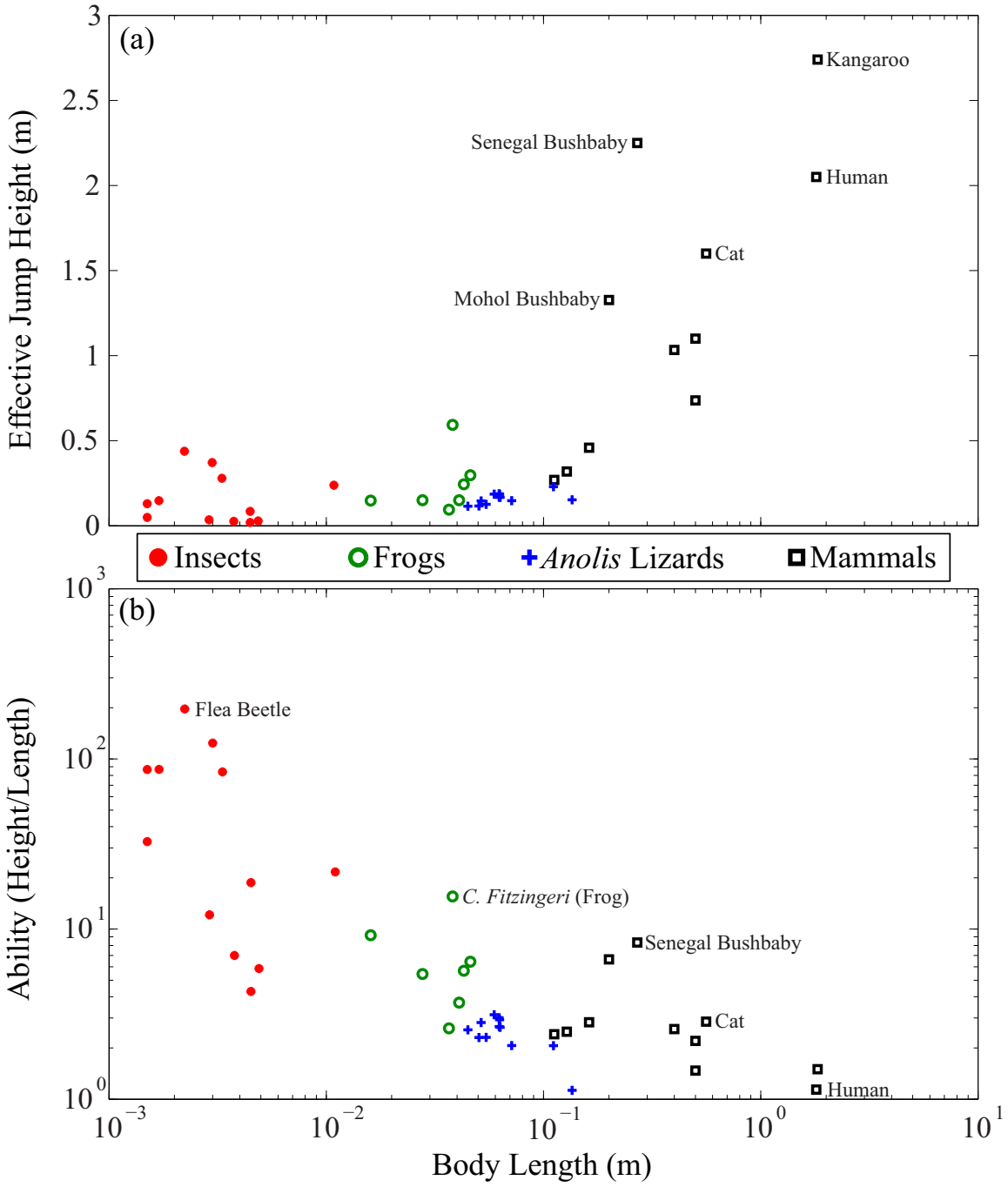

Figure 2: Comparing the jump performance of different sized animals. (a) Effective jump height vs. size. (b) Jumping ability vs. size.

Yet, when considering jumping ability, or jump height relative to body size, the relationship is inverse to body size (Figure 2(b)). Among six species of Anurans

(frogs), size was inversely correlated to relative jumping distance [99]. Similarly, Zug also found that, while absolute jumping distance increased with snout-vent length, relative jumping ability decreased with snout-vent length [122][123], which suggests that, to truly increase jumping ability with increase in size, it is not sufficient to proportionally scale the gross size of an animal. Interestingly, the values related to this inverse relationship varied widely among different species. Particularly, amongst different species, there were acute performance differences depending on the species' natural habitat; arboreal frogs were the best jumpers, and terrestrial ones were the worst. This perhaps was due to arboreal frogs possibly being morphologically adapted to jump longer distances between trees. Rand's findings support this since it found that there was positive correlation between relative hind limb length and jumping ability; arboreal frogs had moderately long legs relative to body size and high jumping ability, whereas the terrestrial frogs had the shortest legs and poorest jumping ability [99]. Further evidence supporting the effects of morphology on jumping performance in frogs was found in a set of take-off experiments with 7 Anuran species in which both relative leg muscle mass and relative hind leg length, which together characterized contractile potential, correlated positively with take-off velocity [34]; though some studies found no correlation between hind limb length and jump performance [39][62]. Additionally, amongst the arboreal species, high tree jumpers were found to be worse jumpers than those that jump on grass reeds. For primates, branch compliance may be too large to be advantageous in locomotion, and instead increases energy cost of arboreal locomotion [9]. Similar principals may apply with grass reed dwelling frogs, requiring them to compensate with increased muscle mass.

The effect of morphology on jump performance has been found in other animals as well. Both hind limb length and lean extensor muscle mass relative to body mass have strong positive correlations with take-off velocities in cats [51]. In *Anolis* lizards, hind limb length, forelimb length, and tail length all correlated with jumping

distances in 15 different species [73]. Yet, since there were also strong correlations in these morphological traits with body size for these species, a phylogenetic and statistical analysis was performed which found that the evolution of hind limb length was associated with evolution of jumping ability regardless of the effect of body size.

Yet, even with relatively large appendages and increases in muscle mass, the power produced by these propulsive muscles do not explain the overall power output produced by animals during a jump [40]. In fleas, for example, jumps are created through impulsive forces that have a duration of only 0.75 ms, while the latency in the muscle is on the order of 3 ms, making it impossible to generate sufficient power and propel the jump through means of conventional muscle forcing [17]. Similarly, in locusts, maximum power output of each extensor tibiae muscle is 36 mW, while the max power output of the jump is about 0.75 W, or a tenfold power amplification [16]. The *Galago senegalensis* (bush baby) has an excellent jump capability of 2.25 m or six body lengths. Assuming constant acceleration during push off, Bennett-Clarke [16] estimated a power output of 2350 W kg^{-1} for the bush baby. He inferred that, due to the fact that this value was far higher than typical values for theoretical maximum powers in muscles (such as 371 W kg^{-1} in frog hind limb muscles [75]), power amplification occurred in bush babies [18]. This was later confirmed through experimental measurements [47]. Thus, many animals must use power amplification mechanisms to propel their jumps.

1.2.3 Elastic Energy Storage

Power amplification in jumps results from energy storage in elastic elements in the appendages responsible for jumping. In vertebrates, this elasticity is largely found in the tendons, which tend to have uniform properties among many mammalian species, with a nearly constant tangent modulus of elasticity of 1.5 GPa for stresses greater than 30 MPa [20]. The tangent modulus of elasticity is an estimate of Young's

modulus where the stiffness used in the modulus calculation was approximated from force vs. displacement curves of tensile loading tests on tendons. Tendons have low energy dissipation. When tendons recoil, they dissipate only 7% of the work done when stretched as heat [8]. The energy that can be stored from tendons has been well documented in other animals [82] and was found to be up to 52 J in humans while jogging [57].

Tendons can have high elasticity. In humans, for example, the main extensor in the foot has a compliant muscle-tendon complex [57]. Hof's study used strain gages, a potentiometer, and a piezo-electric accelerometer to measure moments and angular displacements on 12 humans that bent their ankles in an ergometer. A muscle-tendon complex model was considered that identified two elastic components, one in series (SEC) with the contractile element and one in parallel (PEC). The SEC was identified as the Achilles tendon. Using this model, the measurements were converted to stiffness values with respect to moment. The effective stiffness in the complex was calculated to have an average of 306 Nm rad^{-1} at a muscle moment of 100 Nm, which agreed surprisingly well with Hooke's law estimates using data on Young's modulus and cross sectional areas of the Achilles tendon.

The role of elastic energy storage in improving jump performance is one of power amplification [8]. Muscles are restricted in the amount of power that they can produce, which is determined by the product of muscle force and shortening speed. As the shortening speed increases, the force available decreases [55], with the shortening speed being optimal at around $0.3v_{max}$ [117], and since tendons can recoil at a faster rate than muscles shorten, they can act to amplify power.

This power amplification is evident in dramatic fashion in insects like the flea, which has a catapult mechanism that slowly coils and tenses elastic material known as resilin, while a catch mechanism keeps the legs locked in a flexed position until maximally tensed and then releases all the stored energy at once [17]. This is a

similar concept to flicking your fingers. Bennett-Clarke found the jump height of a rabbit flea to be 4.9 cm, or over 30 body lengths, and a human flea (*Pulex irritans*) of comparable mass was recorded jumping to a height of 13 cm and considered capable of up to 20 cm jumps [17], making fleas among the best jumpers in the world in terms of jumping ability. Similar catapult mechanisms have been found in other insects such as click beetles, flea beetles, and locusts [42][29][54]. And while frogs do not have a catch mechanism similar to insects, their own weight is considered to be a catch mechanism [102]. A frog's hind limb muscles are uncoupled from whole body movement, and as such are able to shorten their muscles and pre-stretch their tendons and store elastic energy before any movement occurs, doing so at a slower rate than if whole body movement and muscle shortening were coupled [102]. This effective catapult mechanism in the frog makes its jumping strategy more similar to insects than to other squat jumping vertebrates.

Other vertebrates, however, have not evolved such catch mechanisms to be able to release stored elastic energy as a catapult, and must instead rely on specific inertial movement strategies to fully leverage power amplification through elastic energy storage. A study in 2003 that examined a theoretical model that consisted of a muscle, compliant element and inertial load in series demonstrated how such as a system could experience power amplification with tendon recoil and is primarily influenced by the amount of inertial loading [44].

The two most common and considered methods for jumping are countermovements and squat jumps. A countermovement is characterized by starting upright, and then quickly squatting and pushing upward. A squat jump is characterized by starting from rest in a squatting position. Alexander developed a theoretical bipedal model of jumping that predicted that animals that produce insect-like ground forces (characterized by high simulation ground forces relative to body weight, $58mg$, m for mass and g for gravity) would benefit exclusively from catapult jumping, which

has been found to be a common method of jumping in insects [5]. In animals that produce bushbaby ($12mg$) or human-type ground forces ($2.3mg$), countermovements and catapults would both achieve greater jump heights than squat jumps, catapults more so in bush baby type forces. The countermovement causes elastic energy storage to occur through passive inertial loading during the preparatory phase, which pre-stretches the muscles and tendons that then recoil and amplify power during the push-off phase.

Indeed, the performance of countermovements and squat jumps have been compared in humans in a number of studies [69][114][67]. The countermovement always performs better than the squat jump. In fact, more than twice as much energy is stored in the tendons during a countermovement than a squat jump [114]. A similar result was found in a study of jumping in *Anolis* lizards, in which the species that performed the countermovement produced a greater muscle mass specific power output than the species that performed a regular squat jump [113]. Many prosimian primates have also been observed performing countermovements [48][37][36][1] among which includes the *Galago senegalensis* (bushbaby). In bushbabies, elastic energy storage does not only occur during the preparatory phase of the jump, but also during the early push-off phase. The energy is then suddenly released at take-off. Thus, it is suspected that the bush baby performs some combination of a countermovement, squat jump and catapult [1]. The countermovement is so pervasive among prosimian primates that it is performed without discrimination of substrate. It was observed in vertical jumps in both natural environments on compliant branches [36] as well as in a laboratory setting on rigid force plates [48], and even by clingers that jump horizontally off of tree trunks to other trunks [37].

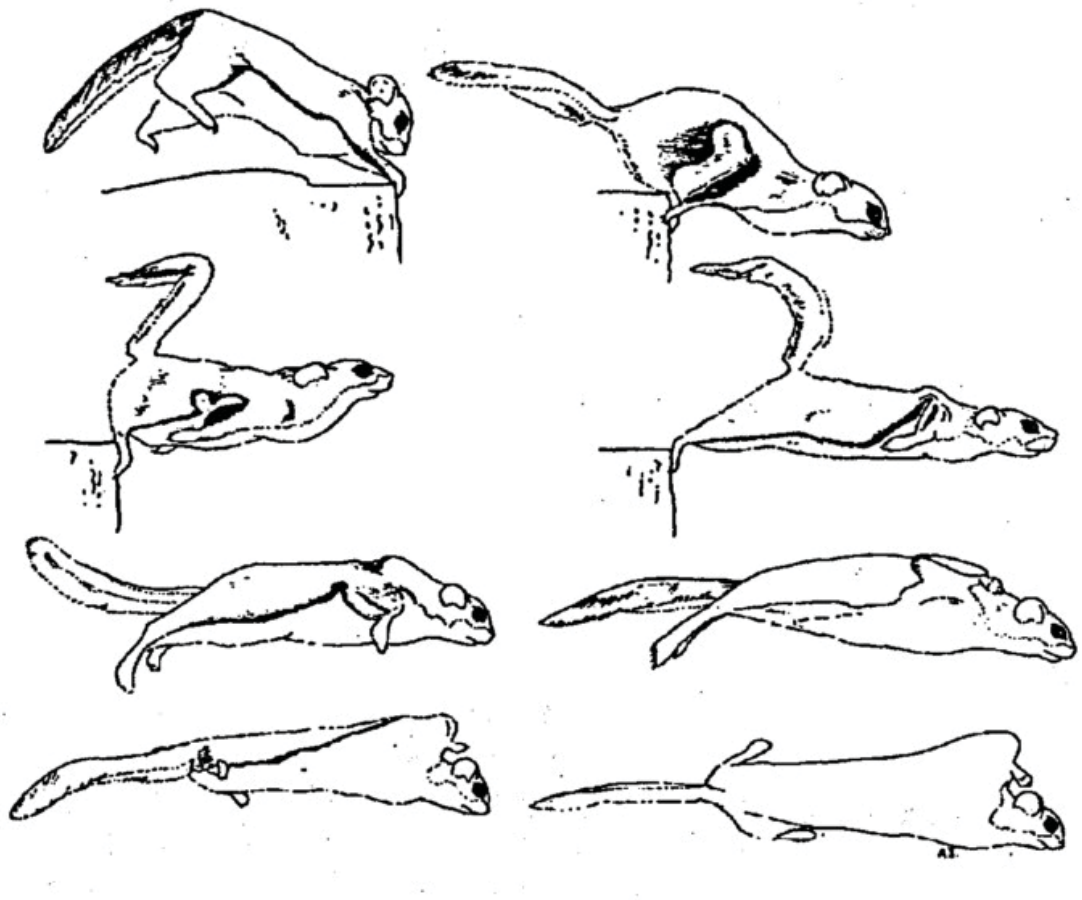

Figure 3: Illustration of the jump sequence of a flying squirrel [63].

Similar principals of elastic energy storage have been used to explain the efficient hopping gait of various marsupials [22][64][7][23]. A particularly interesting version of the countermovement that has been observed in some species is a preparatory hop preceding the countermovement. In our study, we call this movement a stutter jump. Demes' study reported this behavior for all four species of lemurs observed [36]. In Gunther's study, this was observed in the *Galago moholis*' jumps [48]. The stutter jump was also observed in flying squirrels, chipmunks and red squirrels prior to take-off from the edge of a pine board [41][63](see Figure 3). The stutter jump in the animals was so consistent that it was referred to as a "stereotyped preliminary hop". Bush babies may on occasion produce a movement similar to the stutter in

which a jump occurs "out of previous forward motion", which, though not clear, likely suggests a running start, similarly introducing additional momentum to the start of the countermovement [109]. In comparison of jumping versus steady state hopping in wallabies, a "moving jump" was utilized by the animal in which a short-lived hopping gait to the force plate preceded the jump to an elevated platform [80]. The forward velocity of the hopping gait did not differ between steady hopping and jumping.

Table 1: Various animals and their observed jumping strategies

Animal	**Jump Types**	**Stutter?**
Insects (fleas, click beetles, locusts, flee beetles) [46][17][42][54][29]	Catapult	No
Frogs [99][100][123][33][34][102]	Squat / Catapult	No
Anolis Lizards [73][113]	Countermovement, Squat	No
Cats [119][51]	Squat	No
Lemurs (*Avahi laniger, Indri indri, Propithecus diadema, Propithecus verreauxi*) [48][37][36]	Countermovement	Yes
Senegal Bushbabies [109][1]	Countermovement / Squat / Catapult	Yes
Mohol Bushbabies [48]	Countermovement	Yes
Humans [56][67][35] [28][48][114][69][58]	Countermovement, Squat	Yes (Volleyball)
Rodents (Chipmunk, Red Squirrel, Flying Squirrel) [63][41]	Countermovement	Yes
Yellow footed rock wallabies [80]	Hop	Yes

In humans, drop jumps, which have similar qualities to the stutter jump, have been compared with the performance of regular countermovements. The drop jump is a countermovement preceded by a drop from a slightly higher platform. In general, the performance of a drop jump is comparable to the countermovement [28], and is better than the squat jump [67]. But whether the drop is actually any better than

regular countermovements is still under debate and seems to vary among men and women as well as males of varying athletic ability[67]. In volleyball, two different jumping techniques are used: a "hop jump", which is a quicker stutter jump while using both feet at the same time, and a step close approach, which is more of a skip, with one foot after the other. Both jumping techniques produced comparable jump heights, though the hop jump, which is the quicker and more impulsive approach, required greater muscle effort [35]. Another drop jump study uncovered how a proper prelanding angular velocity of the knee joint in which a larger knee flexion just before landing would produce a bouncing type drop with greater take-off velocity [58] (see Figure 4). These findings seem to suggest that the movements involved in the stutter jump must be precisely timed to achieve a mechanical and energetic advantage over a regular countermovement.

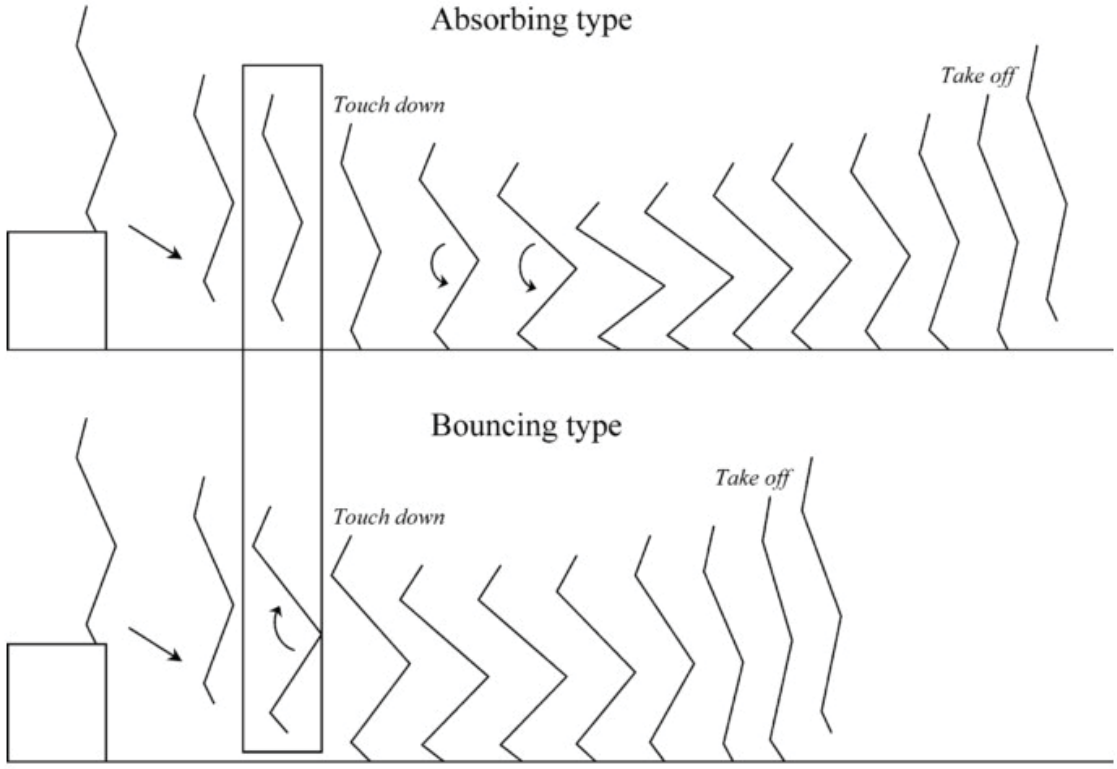

Figure 4: Illustration of two type of drop jumps [58].

1.3 Jumping Robots

1.3.1 Biological Inspiration

In robotics, biologically inspired designs have resulted in machines that are better able to traverse diverse terrain than wheeled vehicles. Animals are regularly tasked with maneuvering in highly complex environments, and it can be argued that they have evolved to become adapted to these challenging environments in ways that conventional technologies cannot rival. Particularly, wheeled vehicles are the accepted standard of terrestrial locomotion using conventional technology. It is a method that is effective at traversing smooth terrain that is not characterized by jagged changes in altitude, but can fail when confronted with large obstacles. Armour *et al* [13] and Sayyad *et al* [104] provide extensive reviews of robots that researchers created which utilize hopping and jumping strategies. Sayyad *et al* highlight the advantages as well as the challenges with using hopping gates versus wheeled solutions in robotic locomotion. They argue that legged locomotion can be superior in that it can allow for active body suspension, isolated footholds, and generally deal less damage and obstruction to the environment when compared with wheeled vehicles [104]. Most importantly, however, legged robots are capable of more complex maneuvers and thus have increased adaptability to uneven and complex terrain.

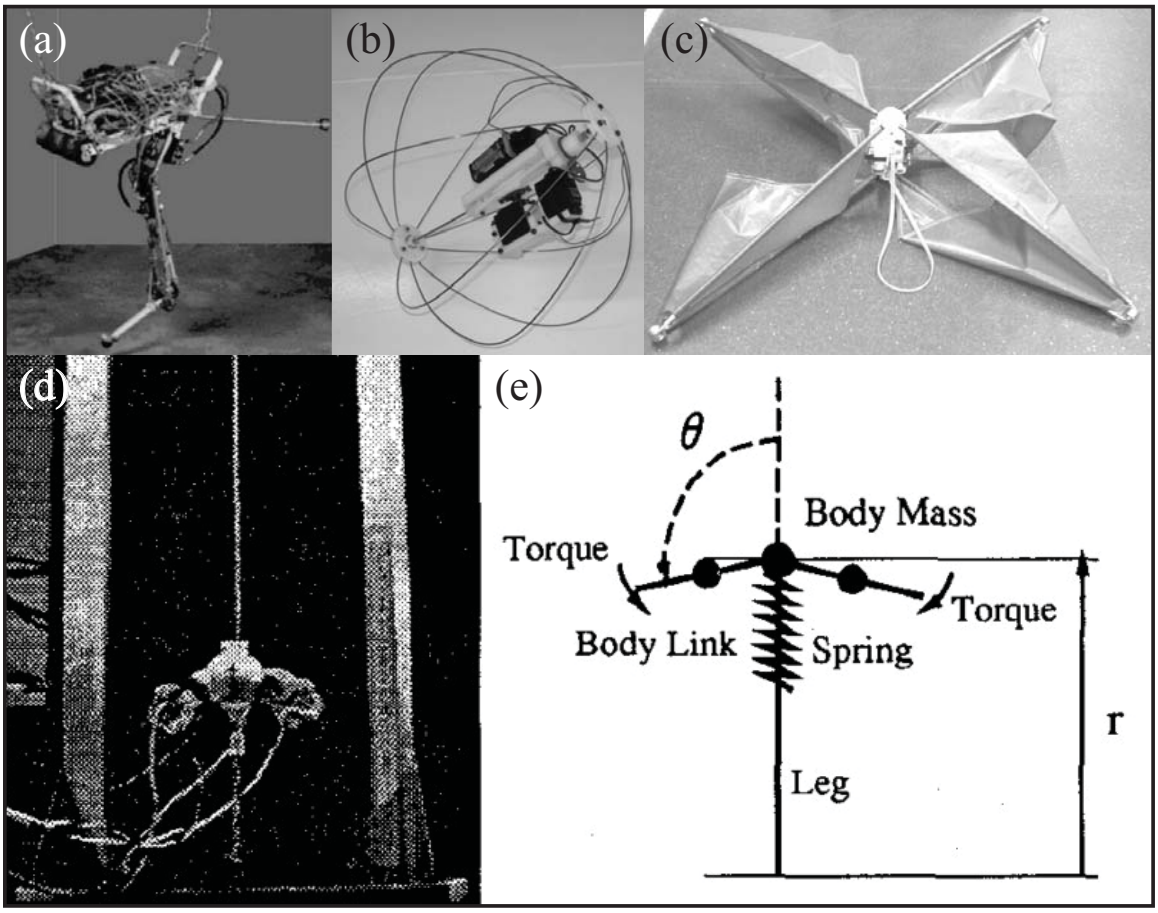

Figure 5: Biologically inspired robots. (a) Uniroo [120]. (b) Jollbot and (c) Glumper [13]. (d)(e) Arm swinging robot [88].

Researchers have developed interesting robotic interpretations of animal jumping and hopping mechanisms. The Uniroo was a 3-leg-link hopping robot based on kangaroo locomotion, with a soleus spring arrangement [120] (Figure 5(a)). Using hydraulic actuators, the hopper was able to achieve over 40 hops in a given trial. Armour and researchers developed two jumping robots that utilized the catapult jumping mechanism: Glumper and Jollbot [13] (Figure 5(b) and (c)). As the name would suggest, the Jollbot, inspired not only by the catapult jumping mechanisms seen in various insects and frogs, but also the rolling ability of certain organisms like the web-toed

salamander and tumbleweed, used a combination of jumping and rolling for locomotion, in which the rolling mechanism also worked to orient the direction and angle of jumping. The Glumper, inspired by the gliding capabilities of flying squirrels, used four legs surrounding the top and bottom of its exterior body with two leg links each to jump using a catapult mechanism and subsequently glides using the air resistance caused but the sails attached to the legs. Glumper performed better than the Jollbot, jumping nearly 2 m high. One interesting adaptation to hopping robots was the addition of two rotating symmetric arms with masses attached, similar to how humans use arm swing to improve jump height [88] (Figure 5(d)). The robot was able to perform high jumps while hopping in place.

1.3.2 An Engineer's Perspective

Legged robots that can adapt to complex environments also have more complex dynamics than wheeled vehicles, with distinct phases and gaits creating nonlinear behavior. This can pose a challenge to engineers in controlling these robots. Also, wheeled vehicles can carry larger payloads relative to their weight, and in legged robots, greater carrying loads requires larger actuators which in turn increases the carrying load. However, while there may generally be increases in the complexity in legged robots versus wheeled vehicles, the hopper construct by NASA's Jet Propulsion Laboratory (JPL) was developed with the premise that wheeled vehicles for celestial exploration can already have a large number of actuators and linkages, increasing complexity of control and chance of failure [49]. The resulting robot was able to reduce the number of actuators and jump via a catapult mechanism using a six bar linkage, and even had self-righting capabilities after landing.

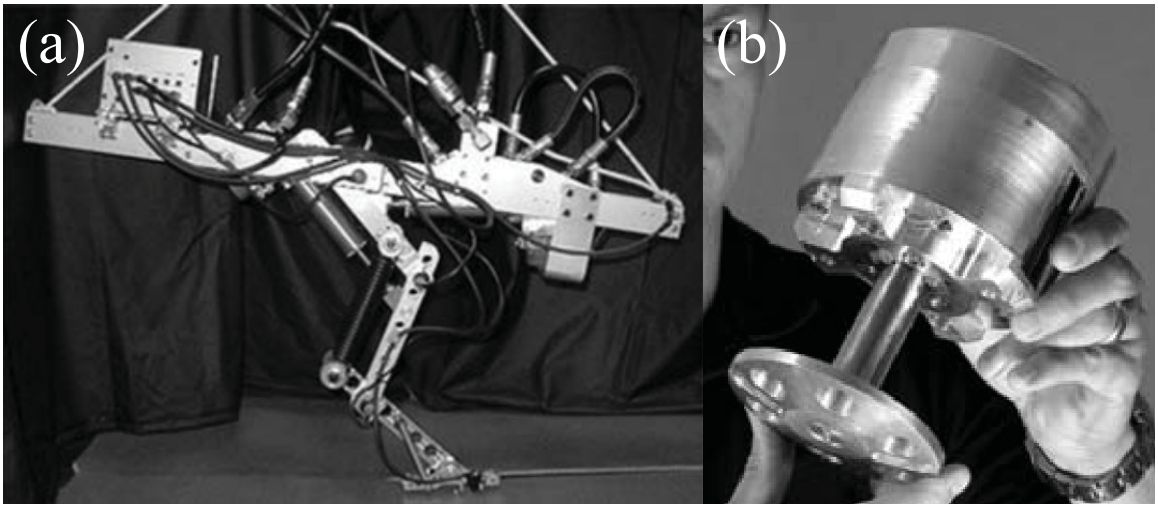

Figure 6: Hopping robots of varying complexity. (a) Kenken [60]. (b) Sandia Hopper [45]

However, posed with these challenges intrinsic to legged locomotion, the focus in hopping robotics has typically been from a roboticist engineering perspective. The intent has not only been to apply a biologically observed physical principal of jumping or hopping, but also of improving designs by tackling these challenges. For example, one of the initial improvements to the design of hopping robots was to change actuation technologies from pneumatic [98] and hydraulic [120] to electric actuators such as small DC electric motors [2] chosen as the cleaner, safer and less expensive alternative while still having high torque-weight ratio [104]. Various researchers have also explored the complexity with which to realize hopping behavior. Such an increase in complexity can be seen in Kenken [60], which was a hopping robot based an articulated 3-link leg, seen in nature (see Figure 6(a)). Hyon and researchers argued that there are practical advantages to an articulated leg such as large clearance between foot and ground, and while there is added complexity compared to a telescopic leg, the structure is simple to build, since it connects two link ends with a rotary joint. Hoppers such as Kenken as well as Uniroo [120], Zhang's Uniped [121], and Berkemeier and Desai's robot had more leg links than most other hoppers [21]. However,

complexity, does not necessarily correlate to performance, as evidenced by Sandias simple telescopic hopper, which was capable of hopping 20 feet in height and about 100 hops on one tank of fuel [45](Figure 6(b)).

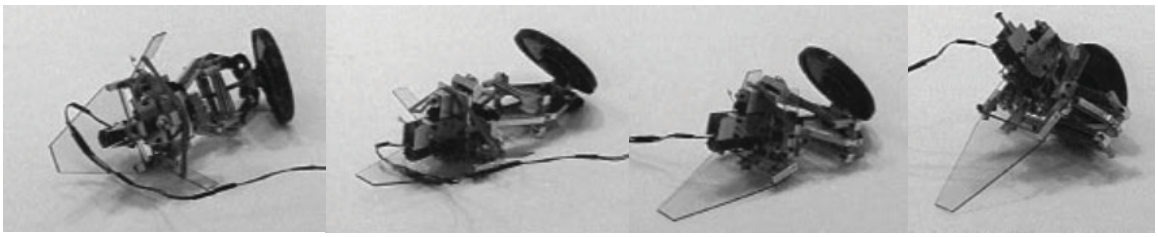

Figure 7: Self-righting sequence of the JPL Hopper V2 [49].

Researchers have strived to make robots that are functional and autonomous. These robots are not particularly made as experimental platforms to learn the fundamental physics behind animal jumping. Thus, relatively few robot jumpers are treated as simple experiments constrained to only move in the vertical direction [88][83][111][95]. Jumping robots typically are allowed to move in 3D [13][105][86], or 2D with a planarizer [91][121][76][21][30]. Even the simplest one-legged, one-link, hoppers have balancing strategies both active [98] and passive [101]. And some robots even have self-righting or orienting capabilities [13][49](See Figure 7).

1.3.3 Robotic Jumping Strategies

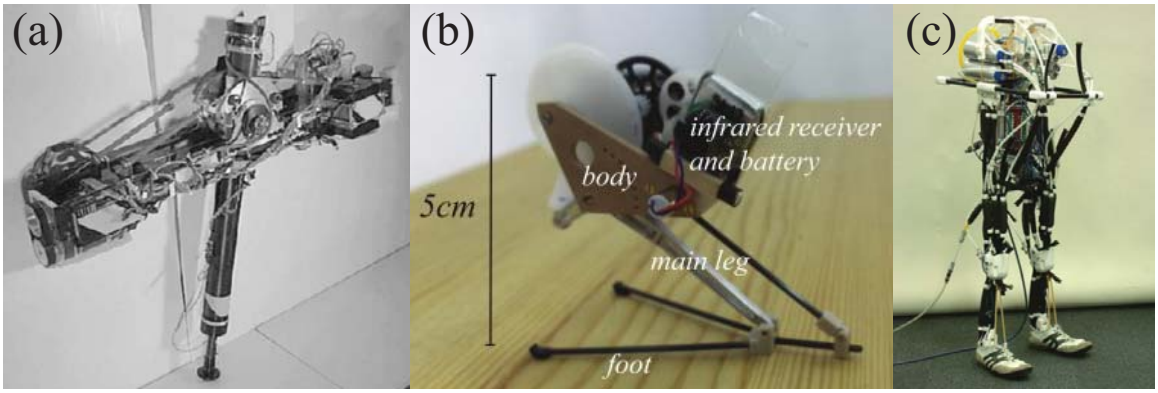

Figure 8: Robots with various jumping methods. (a) Hopping in ARL Monopod II [2]. (b) Catapult in the miniature 7g robot [68]. (c) Squat jump in Niiyama's bipedal robot [85].

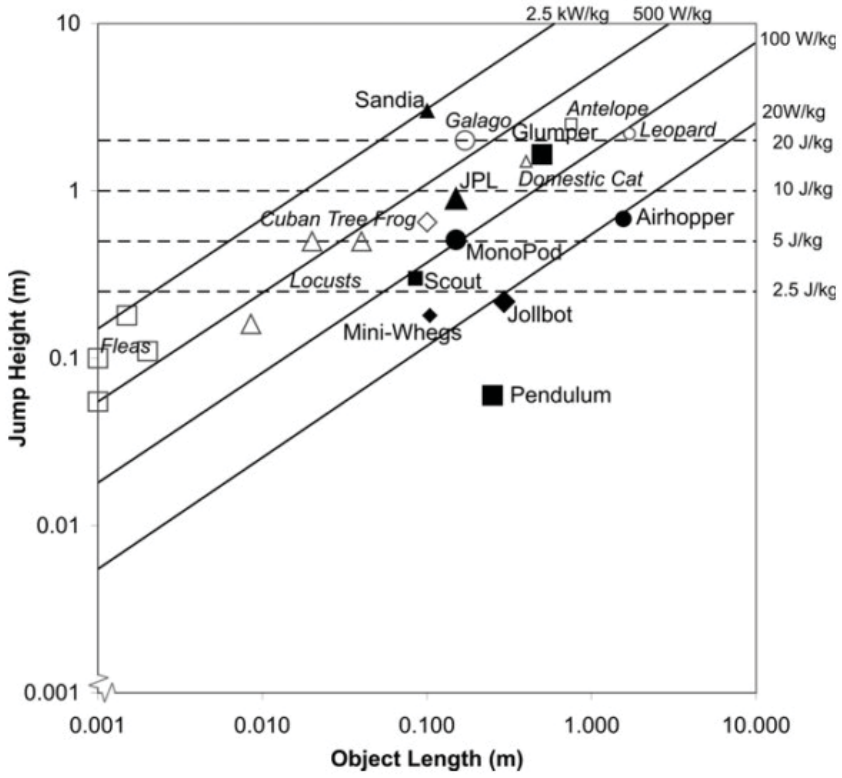

Figure 9: Jump height versus size of various catapulting robots compared with animals [13]

The jumping strategies employed in robots are generally classified as hopping, catapult or squat jump, the last two of which are forms of maximum height jumping (Figure 8). There are many designs that use the catapult mechanisms often seen in insects [107][110][13][105][49][12][84][68]. The jump heights of many of these catapulting robots have been compared with animals (see Figure 9) and have a similar positive correlation with body size as in Figure 1. The large majority of the jumping robots that exist are hoppers (see Table 2). Hopping is a qualitatively different mode of locomotion than maximum height jumping, since maximum height jumping produces much higher power output than in hopping gaits [80]. While the work of this thesis focuses on maximal height jumping, it is important to highlight hopping robots, since the hopping gait stores tendon elastic energy through body movements like the squat jump and countermovement. Additionally, hopping robots tend to have simpler and smaller designs than the squat jumping robots, which can be bipedal and have as many as 4 leg links, based on animals such as humans and dogs [85][86][14]. These simple designs can be beneficial to consider for an experimental study on the fundamentals of jumping.

1.4 Theoretical jumping models

1.4.1 Introduction

Researchers have proposed a variety of theoretical models used to describe and understand different kinds of jumping such as hops and vertical jumps. Mathematical models have been used to express the fundamental locomotive and structural features of jumping. These models range in complexity. Simple models can often explain the underlying properties of jumping in specific manners using fundamental physical principals with a reduced number of parameters. These models make numerous assumptions of the leg structure and physics involved, and as such constrain the models

Table 2: Various robots and their jumping strategies

Jumper	Number of Leg Links	Actuator Type	Jump Type
Balancing Robot [78]	1	Electric Solenoid	Hopping
Raibert Hopper [98]	1	Hydraulic	Hopping
Prosser and Kam [95]	1	Electric	Hopping
Mehrandezh [83]	1	Electric	Hopping
Okubo [88]	1	Electric	Hop in Place
Ringrose Monopod [101]	1	Electric	Hopping
Bow-Leg [30]	1	Electric	Hopping
ARL Monopod II [2]	1	Electric	Hopping
Wei Monopod [115]	1	Electric	Hopping
Sandia [45]	1	Internal Combustion	Hopping
Peck [92]	1	Electric	Hopping
Pendulum [53]	1	Electric	Momentum Based (arm swing)
Takeuchi [108]	1	Pneumatic	Hopping
Uno [111]	1	Electric	Hopping
Scout [107]	1	Electric	Catapult
Akinfiev [3]	1	Electric	Hopping
Dashpod [32]	1	Pneumatic	Hopping
Slip Hopper [103]	1	Electric	Hopping
Rescue Bot [110]	1	Pneumatic and Solenoid	Catapult
Jollbot [13]	1	Electric	Catapult
Grillo [105]	1	Electric	Catapult
Lee Monopod [71]	2	Hydraulic	Hopping
Papantoniou [91]	2	Electric	Hopping
Olie [76]	2	Electric	Hopping
JPL Hopper V2 [49]	2	Electric	Catapult
Luxo [4]	2	Electric	Hopping
Allison Monopod [12]	2	Electric	Catapult
Mini Whegs [84]	2	Electric	Catapult
Airhopper [65]	2	Pneumatic	Hopping
Acrobat-Like [70]	2	Pneumatic	Hopping
Ohashi [87]	2	Electric	Hopping
Glumper [13]	2	Electric	Catapult
Miniature Hopper [68]	2	Electric	Catapult
Uniroo [120]	3	Hydraulic	Hopping
Zhang Uniped [121]	3	Electric	Hopping
Berkemeier [21]	3	Electric	Hopping
KenKen [60]	3	Hydraulic	Hopping
Niiyama [85]	3	Pneumatic	Squat Jump
Mowgli [86]	4	Electro-pneumatic	Squat Jump
Biarticular Bot [14]	4	Electric	Squat Jump

to describe a particular type of jumping. Such models are not only useful in describing locomotion in animals, but also serve to simplify control of biologically inspired robots [26]. For example, the spring-mass model used to describe running and hopping in animals can be utilized in robotics such that the running gate stabilizes in the presence of disturbances without having to actually sense and actively adjust for such disturbances [26]. Simple models are often called templates (Figure 10) and can be used in more elaborate fashion by treating them as individual features of a body such as legs and leg links to improve modeling accuracy [43]. More complex models have also been studied to solve problems that cannot be considered with a single telescopic leg or 2-link articulation [6] and have also been used to understand the role of specific muscle groups [89][112].

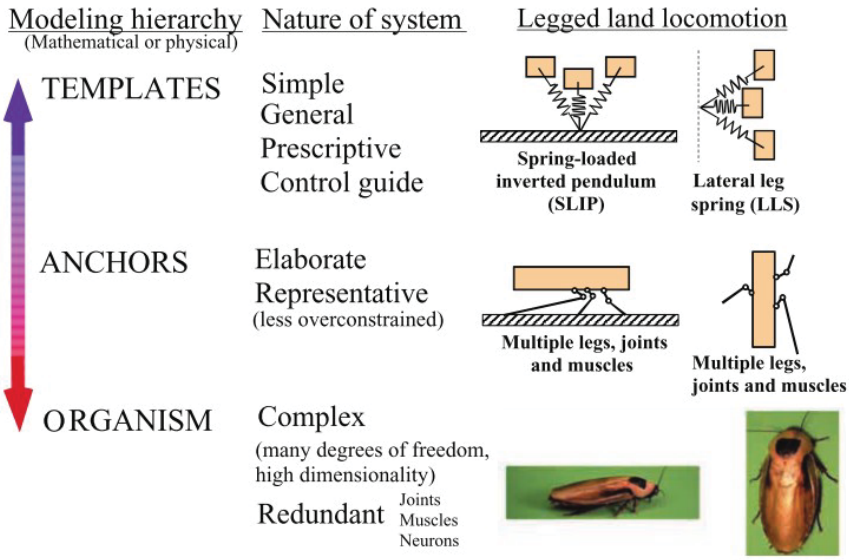

Figure 10: Illustration of template models [43]

Physical models can also be useful in not only verifying mathematical models, but also in performing experiments that are not feasible in animals [6]. For example, McGeer verified the predictions of his mathematical model of bipedal walking by constructing a physical passive walker, which showed that, when put on a slope

the model would enter a stable un-actuated walking gait [79]. Most models used in jumping are math models, though the mass-spring model has been used extensively in robotics to develop hopping robots as shown in the previous chapter [104]. However, the robots are not generally treated as physical or robotic models, rather more as functional robots.

1.4.2 Hopping

To describe hopping in animals, the model most commonly used is the planar spring-mass model, or the spring-loaded inverted pendulum (SLIP). This model is comprised of a point mass connected to a massless spring in series (Figure 11). Raibert was among the first researchers to consider the SLIP model for hopping and developed theoretical models and prototype hopping robots [97] that inspired a plethora of future one-legged robots [104] as well as further research into the SLIP model. To analytically study Raibert's SLIP hopper, Koditschek and Bühler [66] constrained the planar SLIP model to the vertical dimension and considered the task of maintaining a stable and recurring hopping height through actuation. They analyzed the model using both a linear and a nonlinear spring. Both models clearly demonstrated unique solutions for a stable state in which the domain of attraction is nearly every state. Interestingly, the nonlinear spring model also produced a period-two "limping" gate.

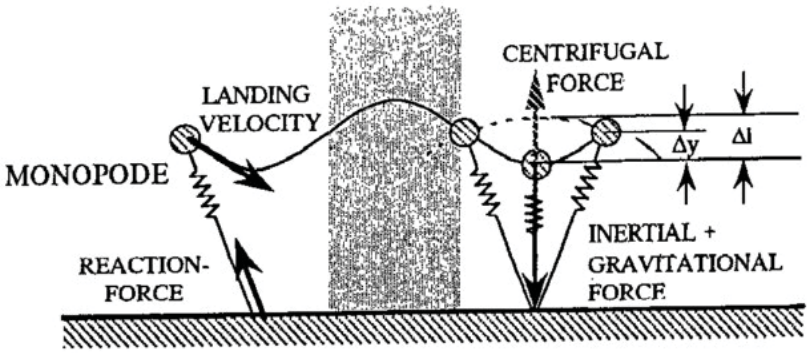

Figure 11: Illustration of the SLIP model [25]

Blickhan used a similar model to study dynamics of both hopping in place as well as hopping with forward motion [24]. He was able to characterize hopping and running based on how measures such as step frequency, contact time, ground reaction forces, and specific power of such gates changed with forward speed. In hopping, the stride frequency remained constant and within a narrow band regardless of forward speed, whereas running gaits have increased stride frequency with speed. Additionally, ground forces were greater during hopping than in running, and there is a positive trend of ground force with velocity. The model showed that even with active forces, bouncing and running systems behave in a similar manner to a simple mass-spring arrangement.

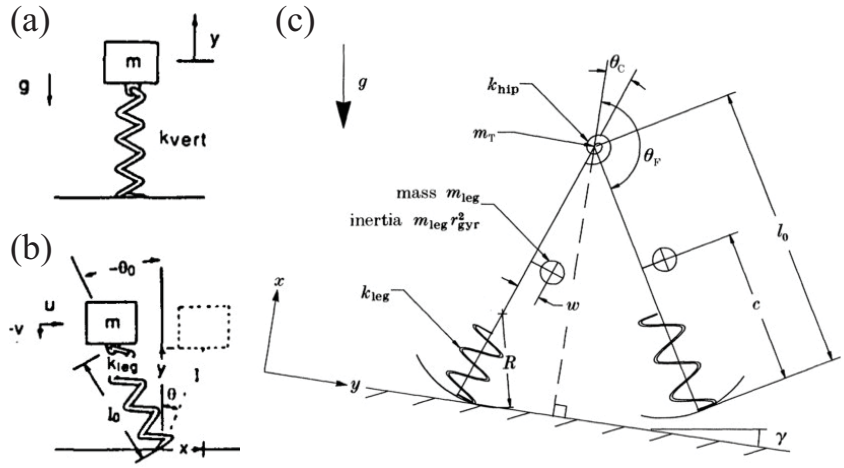

Figure 12: Theoretical hopping models. (a) SLIP as interpreted by McMahon and Cheng [81]. (b) Running biped [79]

McMahon and Cheng also presented a simple spring mass model of running and hopping in animals and made predictions of how stiffness coupled with speed, comparing their predictions with animal data [81]. In previous studies, Cavagna *et al* argued that, during running, elastic energy was stored during mid-step in stretched tendons [31]. With this principle in mind, a model consisting of a mass with a spring leg was presented (see Figure 12(a)) that bounced on the ground according the initial

conditions of the system and stiffness of the leg. Two versions of the model were considered, one in which the model hopped in place, and another in which the model had a forward velocity. From these two models, two effective stiffnesses were calculated, the actual leg or spring stiffness, k_{leg}, and the vertical stiffness, k_{vert}, where k_{vert} was a fraction of the vertical component of the change in ground reaction force and the change vertical displacement. When hopping in place, both values were the same, while when hopping or running forward, the leg lands at an angle, θ_0, and $k_{vert} > k_{leg}$ for any finite θ_0 not equal to 0. The model was iteratively integrated to find the required k_{leg} to have a stable hopping gate. Given the parameters for initial forward and vertical velocity and θ_0, k_{leg} needed to create a gait in which final velocities and θ exiting the ground phase were identical to initial conditions. The parameter space was swept within values reasonable for animal comparison. When compared with animal data of dogs, a rhea and a human, assuming constant leg stiffness, the model accurately described how stride length and step length increased with speed in bipeds and quadrupeds.

A number of researchers have used and elaborated on the SLIP model to compare the 1-legged SLIP model with multi-legged organisms. McGeer elaborated on the simple mass spring system for bipedal running by adapting the model with two legs (Figure 12(b)), each with a mass and spring in series and a curved foot connected to the bottom end of the springs [79]. These legs were connected at a hip joint with a point mass and a torsional spring. Running was a passive mode in this model. Blickhan and Full compared the planar spring-mass monopode model to the dynamics of the hop, trot and running gates in a diverse cross-section of animals with varying numbers of legs [25], and found that the simple model provided a good approximation of those dynamics. Increasing pairs of legs acting simultaneously increased the whole body stiffness in the virtual monopode, increasing natural frequency and stride frequency. Raibert considered the control algorithms for the one-legged SLIP model for

generalizing to multi-legged systems [96]. Four-legged gaits that step with one foot at a time could use the single-leg SLIP algorithms for each leg. Gaits that use two feet simultaneously such as trots, paces, and bounds were represented with a virtual leg.

1.4.3 Maximal Jumping

This section discusses all non-hopping jumping models in which the goal of the jump is maximal height or distance. Many of the models focus on various types of athletic jumps performed by humans, and are all generally more complex than the SLIP model used for hopping. For example, Yeadon's model of the human body was considerably more complex than the telescoping SLIP model [118]. This model was used to explain the twisting and somersault moves in divers and trampolinist athletes. It comprised of 11 segments and 10 joints, requiring 66 equations of motion. Hatze presented another complex 2D human model to study long jumping composed of 17 segments controlled by 46 major muscle groups [52]. The control scheme for long-jumping was optimized in this study. A high jumping model [59] was also developed which, in this case, was actually fairly simple. The goal was to find the minimum kinetic energy requirement to clear a given height in which every point on the body clears the height. The model was a long rectangular rod (Figure 13(a)), mimicking the general length characteristics of a human body. The result of this study was an expression that described the height cleared by an object based on its initial conditions as well as its shape size and inertial parameters. They found that, for a given initial amount of energy, the maximum height cleared would be less for objects with larger moments of inertia.

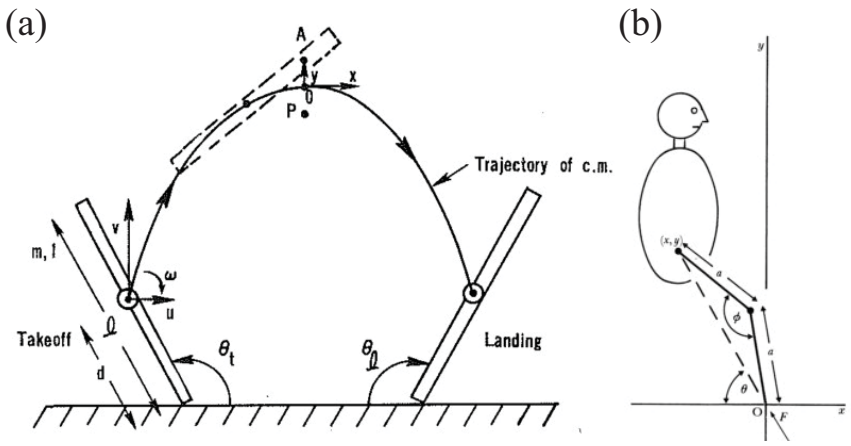

Figure 13: Theoretical high jumping models. (a) Hubbard and Trinkle [59]. (b) Alexander [11]

Alexander introduced a model of jumping that was used to study both long jumps and high jumps [11]. The model consisted of a rigid trunk connected to a two-segment leg that bends at the knee (Figure 13(b)). He used Hill-type muscles [55] for actuation of extensor muscles that were in series with compliant tendons. With this model, he was able make predictions for the optimal movement methods for take-off to achieve both high jumps and long jumps. High jumpers must approach the jump with moderate speed and land the take-off foot at 45° to the horizontal, while long jumpers should approach their jump at the highest speed possible at a steeper angle. Seyfarth *et al* expanded upon Alexander's model by incorporating a more realistic version of the muscle-tendon complex for the knee extensor muscle [106]. The muscle had in-series tendon compliance as well as compliance in parallel to the muscle actuation. And the muscle itself had the Hill-type force-velocity relationship in addition to eccentric forces, or forces due lengthening contraction that work to decelerate a moving joint. The performance of the jumping benefited from the enhancement of eccentric forcing and was in agreement with experimental jumping performances.

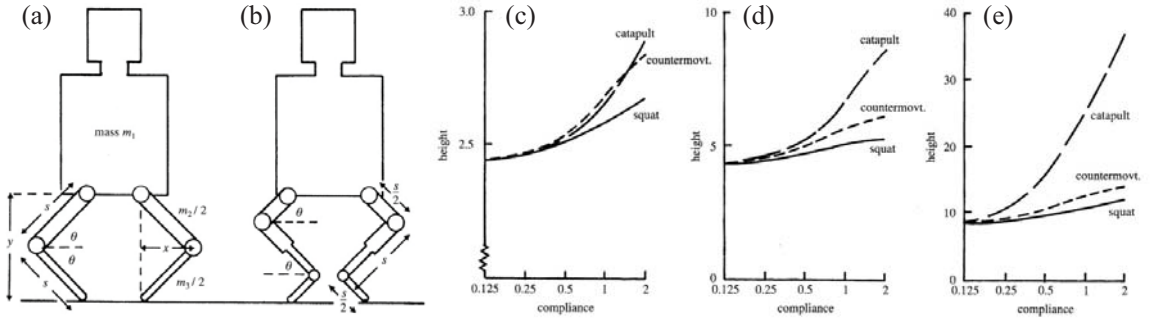

Figure 14: Theoretical model of standing bipedal jumps [5]. (a) Two-link model. (b) Three-link model. Comparison of different jump strategies with (c) human-like, (d) bushbaby-like and (e) insect-like isometric forces.

Alexander also developed a model to study the performance of various types of standing jumps [5]. In this relatively simple model, a main body mass was connected to two symmetric legs at the hips (Figure 14(a),(b)). Alexander considered both two-link and three-link legs. As in the high jumping model, Hill-type muscles were used with series compliant springs. The parameters chosen resembled values in animals ranging in size from locusts, to bush babies to humans. Parameters such as relative leg masses also needed to be considered. Alexander varied parameters such as compliance and muscle-shortening speed as well as legs with 2 and 3 links. Chief among the results of this study was the comparison of the jumping performance using different jump strategies in animals that produce insect-like forces, bushbaby-like forces and human-like forces (Figure 14(c)-(e)). Amongst all animals, the squat jump was the worst jump regardless of compliance value. For animals that produce insect-like forces, the catapult was the best overall jump. For human-like forces, catapult and countermovement performed comparably. Animals that produce bushbaby like forces benefit the most from catapults, then countermovements. It has been suspected that the Senegal bushbaby performs a combination of catapult, countermovement and squat to produce its jump [1].

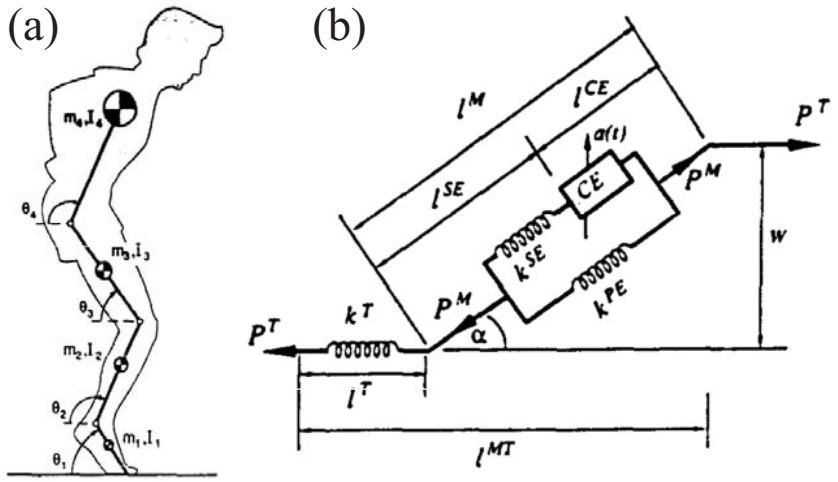

Figure 15: Maximum height jumping model [89]. (a) Schematic of 4-link jumping model. (b) Schematic of muscle-tendon complex model.

Pandy's model [89] for maximum height jumping is more realistic than Alexander's model. The model is planar, consisting of 4 articulated segments driven by 8 skeletal muscles modeled by Hill-type force laws with series and parallel elasticity and elastic tendons (Figure 15). The purpose of this study was to use numerical methods to find an optimal control method for maximum height jumping. The movement strategy was found to be a countermovement, although the countermovement was minimal and was nearly a squat jump, unlike in experimental human jumping results in which the countermovement was more pronounced [90]. Pandy and researchers hypothesized that this incongruence was because the model could not produce strong enough hip moments. A similar model was used by Soest *et al* [112] to understand the role of the biarticularity of the gastrocnemius muscle (GAS) in maximum height jumping. Bobbert used this model to understand how the elasticity of series elastic elements (SEEs) in the triceps surae affected the performance of maximum height jumping [27]. He found that longer more compliant tendons allowed for greater power output and thus greater jump height.

CHAPTER II

EXPERIMENTAL APPROACH

2.1 Philosophy of Approach

We performed a detailed study of a robotic template based on a simple jumping model to examine the effects of movement strategy on jumping performance. This model is a 1D mass-spring system (Figure 16(a)) with an actuated mass, similar to the SLIP template used in modeling hopping and running. The system was actuated through the control of the position of the center of mass of the main body, x_a, relative to the position of the bottom of the thrust rod, x_p. We did not assume that the thrust rod was massless. We derived equations for the balance of forces in the actuated mass and leg from their respective free body diagrams (Figure 16(b,c)) as $F - m_a g = (\ddot{x}_a + \ddot{x}_p) m_a$ and $-F - m_p g + \alpha(-k x_p - c\dot{x}_p) = \ddot{x}_p m_p$, where k, c, g, m_p and m_a are spring stiffness, spring damping, gravity, rod mass and actuator mass, respectively. The constant, α, is a piece-wise constraint that determines whether or not to consider spring and damper forces according to the aerial and ground phases such that, $\alpha = 1$ when $x_p < 0$, and $\alpha = 0$ when $x_p \geq 0$. Combining these force balance equations and simplifying, the equation of motion for this system can be written as:

$$\ddot{x}_p = -\ddot{x}_a \frac{m_a}{m} - \alpha\left(\frac{k}{m} x_p + \frac{c}{m}\dot{x}_p\right) - g, \tag{1}$$

where m is the total mass. The origin position of the thrust rod, $x_p = 0$, signifies when the spring is at its free length. Since there is no mass on the bottom of the spring foot, the spring can only compress and will be uncompressed when airborne.

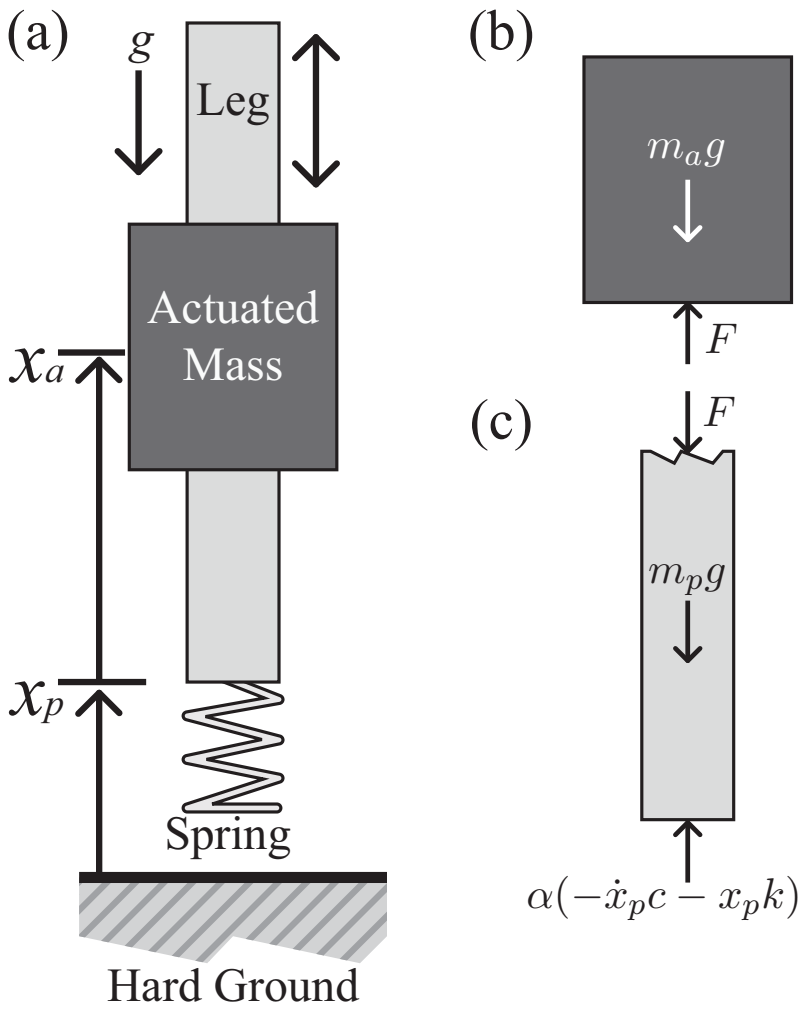

Figure 16: Diagram of the theoretical model. (a) Overall model. Free body diagrams of the (b) actuated mass and (c) leg.

This simple model, which as of yet has only been used to examine steady state gaits such as hopping, allows us to directly correlate aspects of jumping performance to characteristics of such a system, such as overall system resonance. Elastic energy storage allows animals to amplify output power of their jumps. This principle of elastic power amplification has been leveraged in robotics to engineering hopping and squat jumping robots. Thus, the potential benefits of the results of our study are threefold. First, while a more detailed model of jumping in animals would provide a more accurate description, we can use a simple model to form hypotheses of the

factors that determine jumping strategies in different size animals. Second, hopping robots are generally designed according to the SLIP model, and can thus directly apply the findings of our work to perform maximal height jumps. Lastly, the control schemes for more sophisticated bipedal robots may find guidance from our results.

2.2 Apparatus

The robot consisted of a linear motor actuator (Dunkermotoren ServoTube STA11) (see Figure 17(c)) with a series spring rigidly attached to the bottom end of the actuator's lightweight thrust rod (Figure 17). The ServoTube STA11 was a linear actuator that provided a linear force proportional to the current delivered and the magnetic field. Similar to rotational electric motors, the linear motor had a stator and a rotor, except in the linear motor configuration, the stator and rotor were unrolled to produce a linear force instead of a torque. In the STA11, the thrust rod acted as the stator, encasing rare-earth magnets, and the exterior case constituted the rotor that received current to produce electromagnetic fields. The motor included encoders to allow for feedback control of the rotor's position relative to the thrust rod.

The actuator was mounted to an air bearing that allowed for one-dimensional and nearly frictionless motion. However, attaching the carriage of the air bearing added a significant load to the weight of the robot, such that moving the actuator along the thrust rod, and maintaining its position required more power and would heat the motor and amplifier in a matter of seconds when the robot was oriented vertically. To mitigate these effects, the gravitational load was reduced to $0.276g$ by inclining the bearing at $\theta = 75^\circ$ relative to the vertical axis.

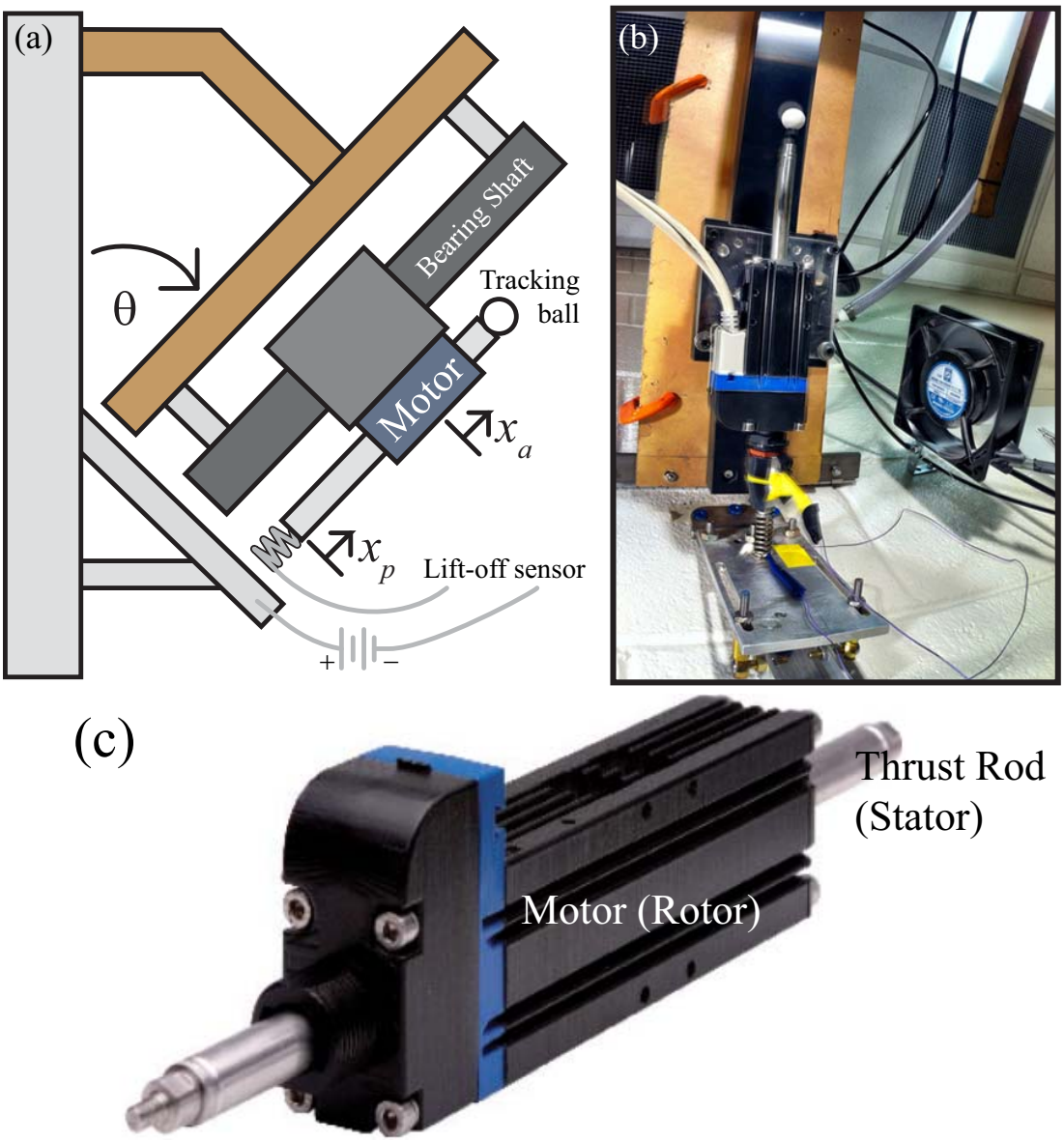

Figure 17: The robot apparatus. (a) Diagram of robotic apparatus, robot was declined to $\theta = 75°$ to reduce motor strain from force of gravity. (b) Picture of robot setup. (c) Close up of the Dunkermotoren ServoTube STA11 motor, image courtesy of Dunkermotoren.

To detect lift-off, we attached a continuity sensor to the bottom end of the spring. The sensor consisted of wire coiled around the bottom of the spring and wire connected the metal base that the robot jumped on. These wires were connected to a USB DAQ

board (National Instruments NI-USB-6009) that supplied a 2.5 V load and measured the voltage of the circuit. When the spring left the ground and disconnected from the metal base, an open circuit was created, causing a change in voltage. The sensor operated at 1000 Hz, allowing the detection of metrics such as time to lift-off from the onset of motor activation and time of flight to 1 msec.

Time of flight was used to measure jump height, derived from the equations of projectile trajectory. The vertical position trajectory in time, $x(t)$, of an airborne object is $x(t) = x_0 + \dot{x}_0 t + 0.5at^2$, where the initial position is $x_0 = 0$, and the acceleration, a, is gravity, $-g$. The velocity of the object at maximum height occurring at time, t_h, is $\dot{x}(t_h) = \dot{x}_0 - gt_h = 0$. Thus, the initial velocity, $\dot{x}_0 = gt_h$, can be substituted into the position equation, which is at maximum height at time, t_h, $x(t_h) = h = gt_h^2 - 0.5gt_h^2$. Since the time at maximum height, t_h, is half of the total flight time, t_f, the equation of jump height can be simplified and expressed as $h = \frac{1}{8}gt_f^2$.

The lift-off sensor, motor control as well as video tracking of a white ball were coordinated through computer with various LabView programs (Figure 18(a)). The motor had feedback control through an Accelnet amplifier (Figure 18(b)). A user-defined position could be commanded with a trajectory method supplied by Copley Controls such as a profile trajectory or a smooth trajectory. We were also able to directly control the trajectory by supplying the amplifier with a list of time step durations, positions and velocities. We used this method to generate sine wave trajectories of the form $x_a = A\sin(2\pi ft + \phi)$.

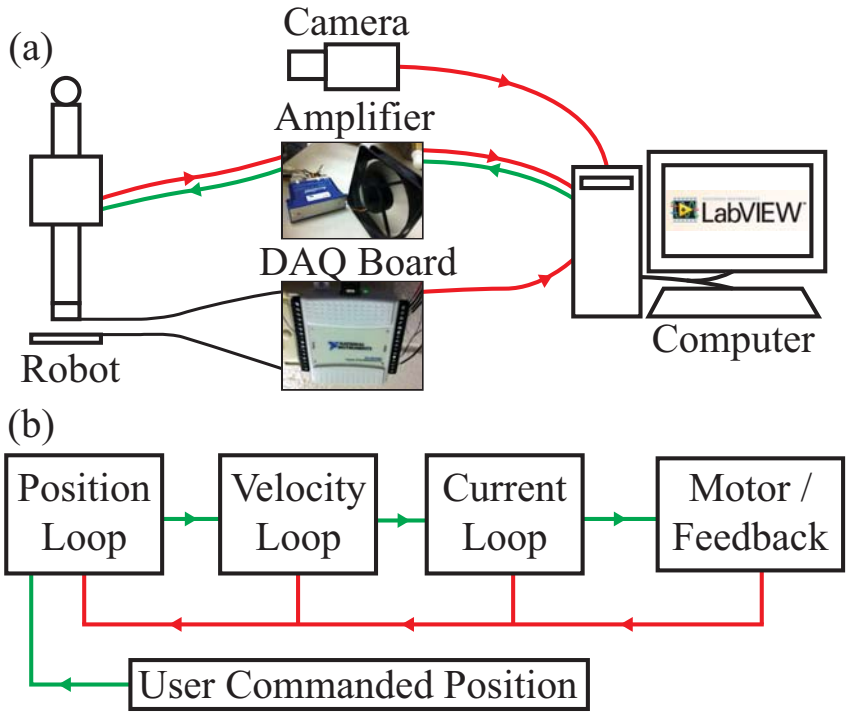

Figure 18: Motor Control and Data Acquisition. (a) Schematic of data communication to and from computer. Labview logo courtesy of National Instruments (b) High level block diagram of feedback motor control loop

We controlled the motor position with proportional feedback and feed forward gains for position and velocity that determined the command current sent to the motor. Most of the gain values supplied were sufficient to control the motor trajectory with the exception of the position proportional gain, which was tuned. Figure 19(a) illustrates the commanded versus actual positions as collected from the amplifier for a relevant range of forcing frequencies. Reducing the value of the position feedback gain to 6% of the value for optimal control damped the entire system, which allowed for much faster automation of experiments by instantly eliminating spring vibrations after a run of a particular jumping experiment.

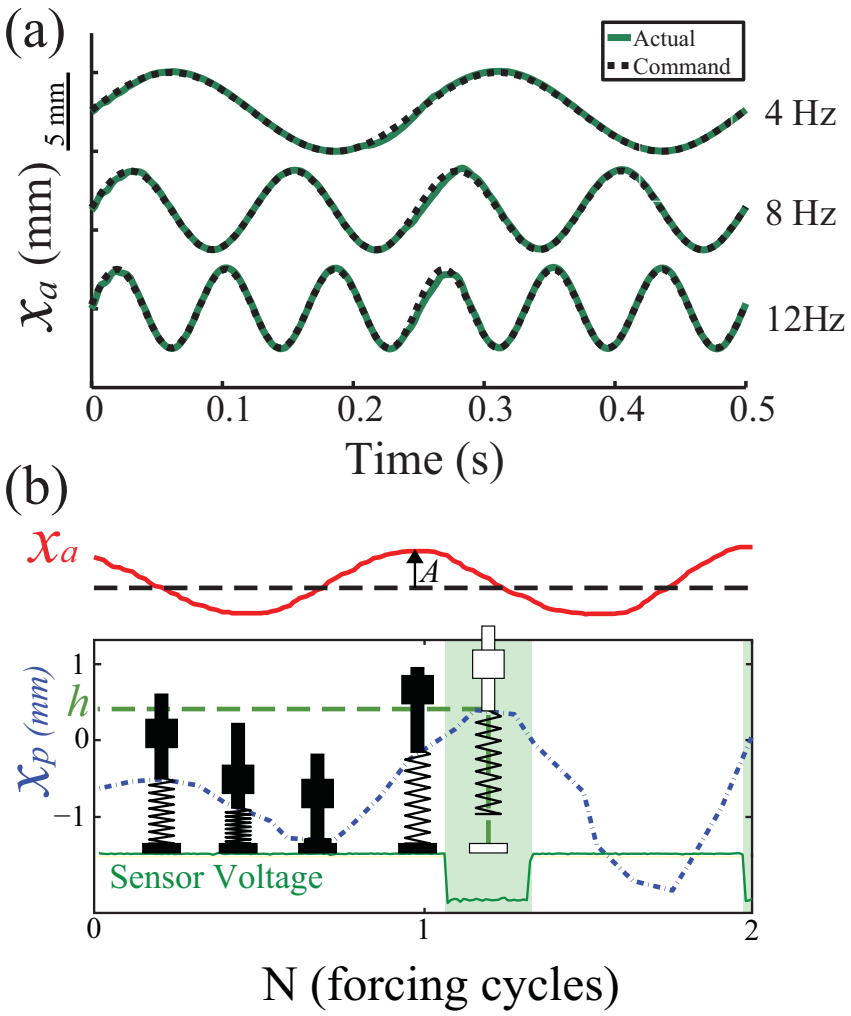

Figure 19: Controllability and data collection. (a) Commanded vs. actual relative actuator position x_a as measured from encoders. The motor was controllable for a wide range of forcing frequencies. (b) Actuator position x_a and video tracked position of the thrust rod x_p, and the lift-off sensor voltage with a sinusoidal forcing amplitude of $A = 0.30$ mm in which the robot lifts off.

The camera used for video tracking was an Allied Vision Technologies Pike camera with a 1394b firewire connection to the computer, capable of 200 FPS video for real-time tracking. To track the 15 mm diameter white plastic ball attached to the thrust rod, the initial search window was established before an experiment by selecting a rectangle around the ball in an initial test image (Figure 20). A routine programmed

in Labview would then determine the centroid location of the ball in a black and white threshold image. For each successive frame of tracking, the software uses the previous frames centroid location to determine the center of the search window. Oscillations smaller than 30 microns were detected.

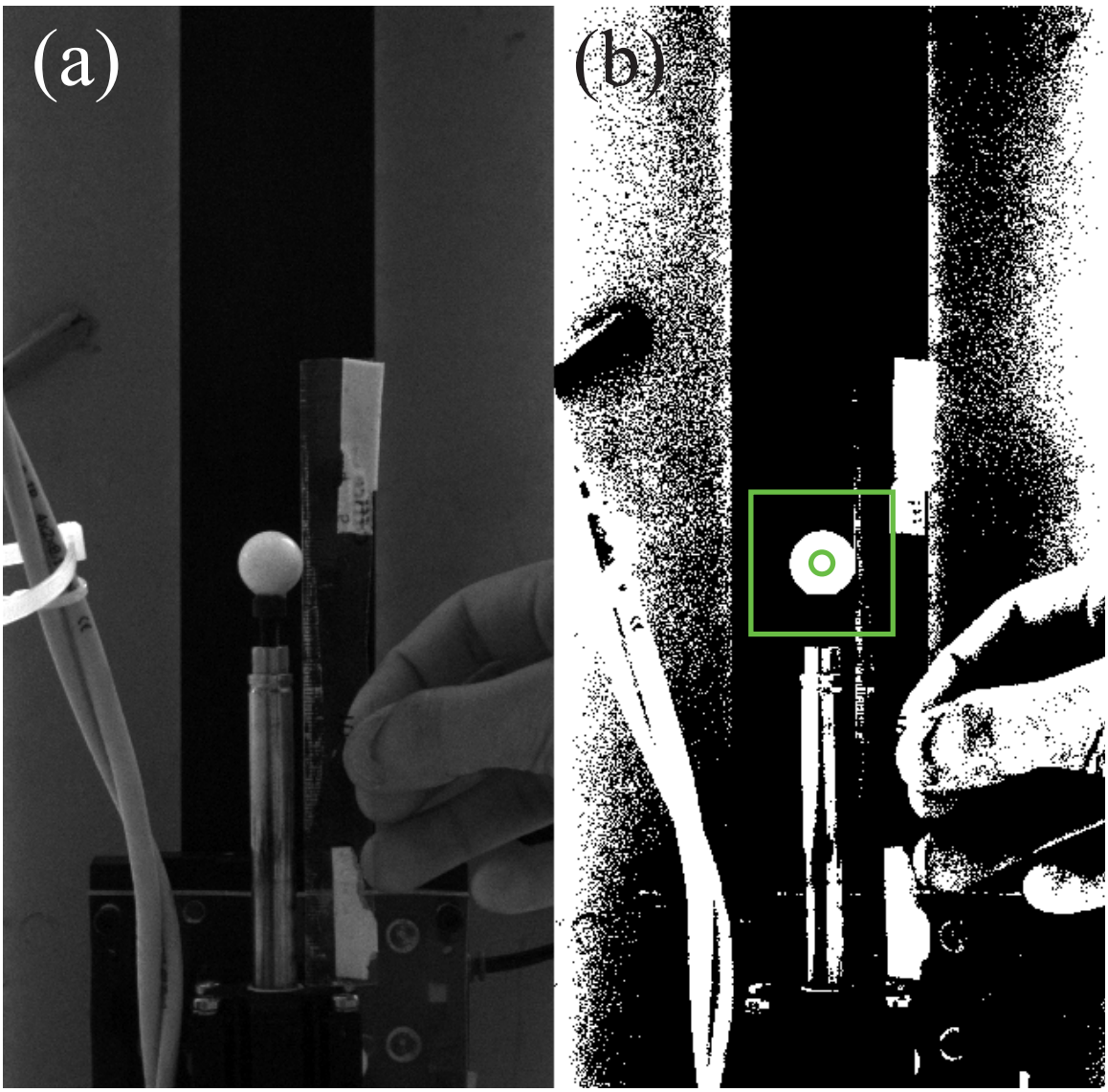

Figure 20: Sample video tracking image. (a) Raw image taken for calibration. (b) Sample threshold image. Green rectangle indicates initial tracking window; green circle indicates white space centroid location.

An example of the coordination of video-tracking, lift-off sensing, and motor control is illustrated in Figure 19(b). Lift-off is detected when there is a drop in the voltage of the continuity sensor. Video tracking was also used to characterize the damping of the spring (Figure 21(b)). From rest, with the relative motor position remaining constant, the robot was lightly excited by a slight tap while on the ground, and the high-speed camera (Allied Vision Technologies) captured the resulting free spring vibrations by tracking a white ball at the top of the thrust rod with software generated in LabView. Camera tracking was also used to determine the coefficient of restitution (0.8 ± 0.06) from ground collisions.

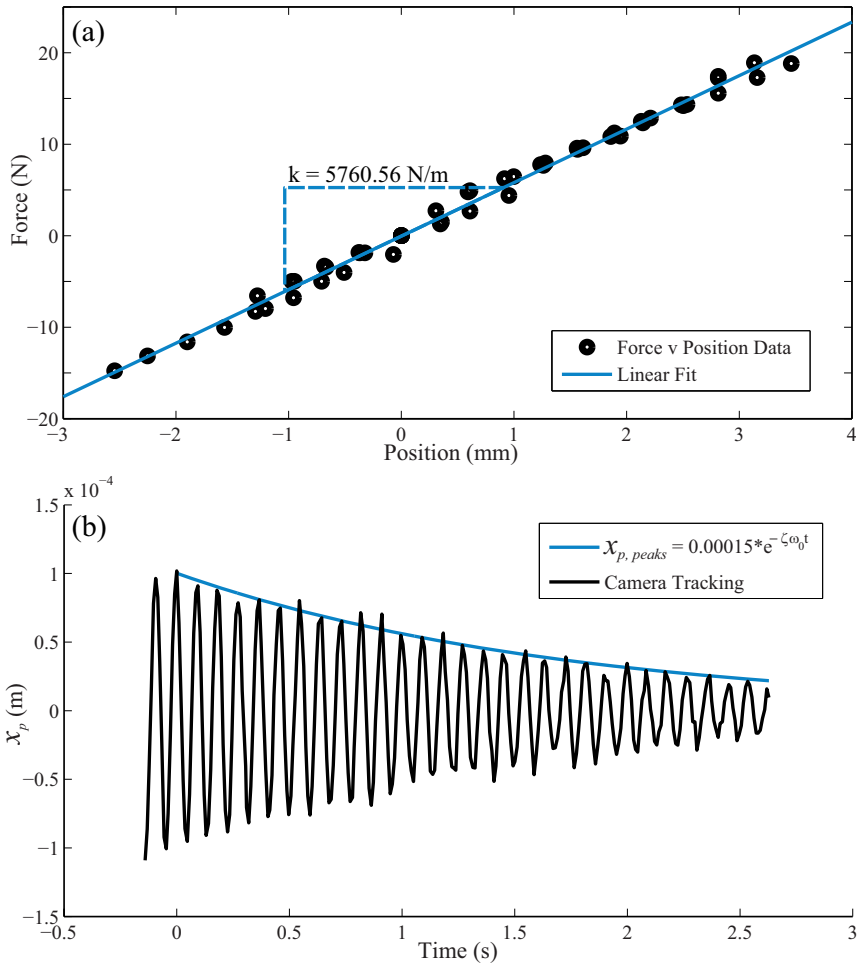

Figure 21: Measuring spring stiffness and damping. (a) Force vs. position data of spring compression. Stiffness was found to be $k = 5760.6$ N/m. (b) Thrust rod position, x_p, during free spring oscillations vs. time. Position re-centered about zero to determine decay equation of oscillation peaks, where $\omega_0 = \sqrt{k/m}$, and damping ratio $\zeta = 0.0083$.

We found the damping ratio to be $\zeta = 0.0083$ by determining the exponential decay of the oscillation peaks. The natural frequency, $\omega_0 = \sqrt{k/m}$ or $f_0 = \frac{\sqrt{k/m}}{2\pi}$, was determined by the overall mass, $m = 1.178$ kg, and the spring stiffness, $k = 5760.6$ N/m, which was determined from force vs. displacement measurements taken by compressing the spring with 6-axis robot arm fitted with a force sensor (Figure 21(a)).

Table 3: Robot Properties

Property	**Units**	**Value**
Total Mass, m	kg	1.178
Motor Mass, m_a	kg	1.003
Rod Mass, m_p	kg	0.175
Stiffness, k	N/m	5760.6
Damping Ratio, ζ	-	0.0083
Damping Coefficient, c	Ns/m	1.368
Natural Frequency, f_0	Hz	11.130
Resonant Frequency, f_r	Hz	11.129

Since the damping ratio is so low, the damping coefficient, $c = 2\zeta\sqrt{mk}$, was also low, making the resonant frequency [15] of the mass-spring system, $f_r = f_0\sqrt{1 - \frac{c^2}{2mk}}$, nearly identical to the natural frequency (Table 3).

2.3 Overview of Experiments

In investigating maximum height jumping performance, we performed two experiments. In both experiments, we commanded the motor to start from rest and then move with a sine wave position trajectory, $x_p = A\sin(2\pi ft + \phi)$, for a specific number of forcing cycles, N. The first experiment was to find the minimum pumping amplitude, A_{min}, required to achieve lift-off for an array of sinusoidal parameters. For a selection of different phase offsets, ϕ, and values of N, as well as a fine sweep of forcing frequency, f, we found the minimum amplitude, A_{min}, required to detect lift-off. The second experiment was to measure jump height for a sweep of f and ϕ at $A = 4$ mm and $N = 1$ cycle.

The following two chapters examine each of these two experiments in detail. Each chapter gives a more in-depth description of the experimental procedure and presents the results.

CHAPTER III

MINIMUM FORCING AMPLITUDE

3.1 Procedure

This first experiment was executed during the beginning exploratory phase of the jumping robot project in which we were examining how to quantify jumping performance in relation to different sine wave parameters. This experiment examined the performance of a jump up to the point of lift-off. For a given frequency, f, phase offset, ϕ, and number of forcing cycles, N, we determined the minimum amplitude, A_{min}, required to achieve lift-off. The robot started from rest at an initial relative position, $x_a = A\sin(\phi)$, and the motor was commanded with a sine wave trajectory with set parameters, A, f and ϕ, for a total of N cycles. After N cycles, with $\dot{x}_a = 0$, we used the lift-off sensor to determine if lift-off occurred at any point. If no lift-off was detected, we selected a higher A for the next run, and vice-versa for when lift-off was detected. We iteratively repeated this procedure in the form of a binary search algorithm that determined A_{min} to within 0.00625 mm, the resolution of the actuator encoders. We determined A_{min} for a range of values of f from 3 to 16 Hz in steps of 0.125 Hz, such that A_{min} vs. f could be plotted and an optimal f could be determined based on the frequency that produced the smallest A_{min}. A total of 8 plots of $A_{min}(f)$ were generated for $N = 1$ and 5 cycles, at $\phi = 0, \pi/2, 3\pi/4$, and π radians (Figure 23).

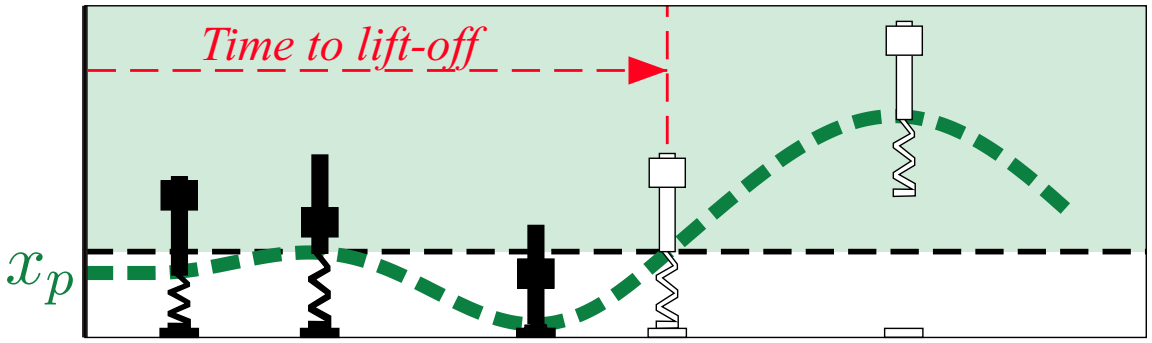

Figure 22: Time to lift-off illustration.

We used a different approach for the experiment in which the time to lift-off was measured. For a given set of sine wave parameters, the motor oscillated for 100 cycles, or until lift-off of was detected, and the time to lift-off was recorded in cycles (Figure 22). At $\phi = \pi$ and $3\pi/2$, we determined cycles to lift-off for over 30,000 combinations of (A,f) (Figure 24).

3.2 Results

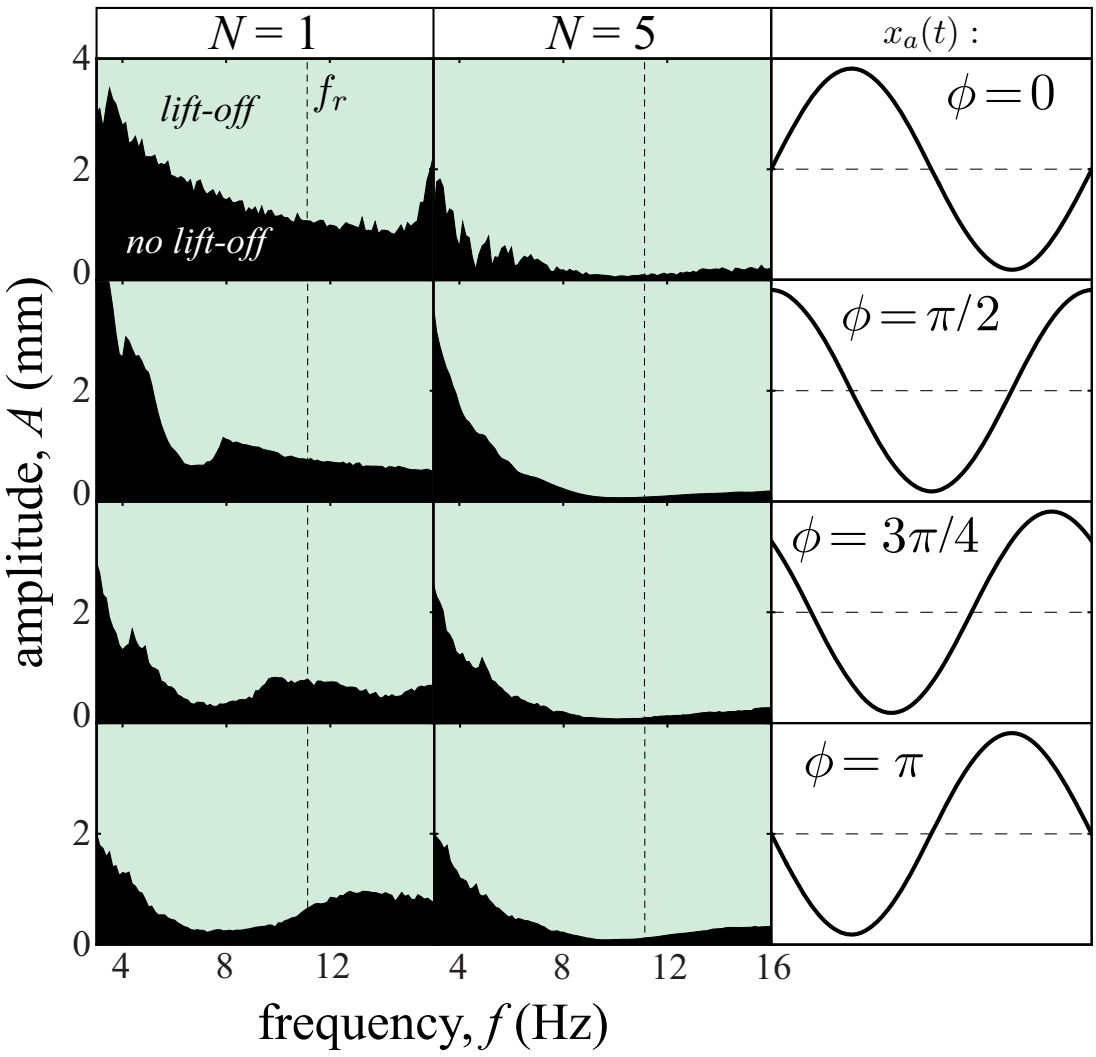

Figure 23: Minimum forcing amplitude. Left and middle columns are plots in the $A - f$ plane that indicate regions lift-off (light blue) and no lift-off (black) when the robot is forced for N = 1 cycle (left column) and N = 5 cycles (middle column) at varying phase offsets, ϕ, indicated by row in the right column. Vertical dashed lines indicate resonant frequency, f_r.

Figure 23 displays the results of the minimum forcing amplitude experiment. If we force the motor for 5 cycles, the optimal f to achieve lift-off was effectively f_r.

However, if the motor was only allowed to oscillate for 1 cycle, then the optimal frequency to achieve lift-off was generally not the resonant frequency and varied with initial phase offset.

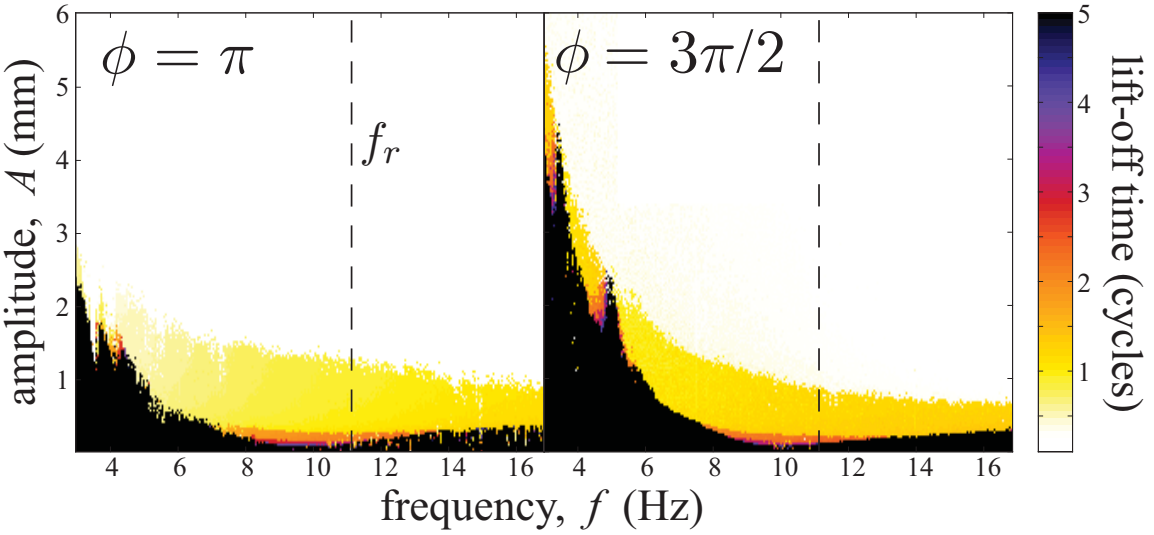

Figure 24: Time to lift-off. Colormap in $A - f$ plane indicates the number of forcing cycles required to achieve lift-off when forced with a starting phase offset, ϕ, of π (left figure) and $3\pi/2$, right figure.

Similarly, measuring lift-off time at different amplitudes and frequencies showed that optimal frequency for lift-off quickly became dependant on ϕ for lift-off times lower than 2 cycles (Figure 24). It should be noted that, for the time to lift-off data presented in Figure 24, we applied a top threshold of 5 cycles to show good color contrast, since the lift-off times quickly reached 100 cycles at amplitudes below the 5 cycle contour.

Interestingly, the dependence of optimal frequency on ϕ became even more pronounced for lift-off times less than 1 cycle. If the robot waited for multiple cycles of forcing to achieve lift-off, any ϕ could be used and resonance was fully leveraged by oscillating the motor at f_r at a very low amplitude. However, it is arguable that the purpose of a jump is not simply to achieve lift-off, but to achieve lift-off quickly or

with a fast take-off velocity to achieve high jump height. Since achieving high jump heights likely requires amplitudes and frequencies that produce transient time-scale lift-off times ($t_{lift-off} \leq 1$ cycle), we hypothesize from the results of this experiment that the optimal frequency for jump height is not necessarily f_r and is dependant on ϕ.

CHAPTER IV

JUMP HEIGHT

4.1 Procedure

To test the hypothesis of the previous experiment, we systematically examined the optimal conditions for maximal jump height for $N = 1$. We fixed A = 4 mm, which was above A_{min} for $f > 3.5$ Hz, and studied how jump height h depended on f and ϕ. Starting from rest at an initial relative motor position, $x_a = A\sin(\phi)$, we oscillated the motor for 1 cycle, past which $\dot{x}_a = 0$. We then measured jump height (Figure 25) according to flight time, $h = \frac{1}{8}gt_f^2$. A total of 6720 combinations of (f, ϕ) for $0.1 \leq f \leq 16.8$ Hz and $0 \leq \phi \leq 1.95\pi$ radians were tested, with 3 trials averaged for each set of parameters for a total of 20160 experiments.

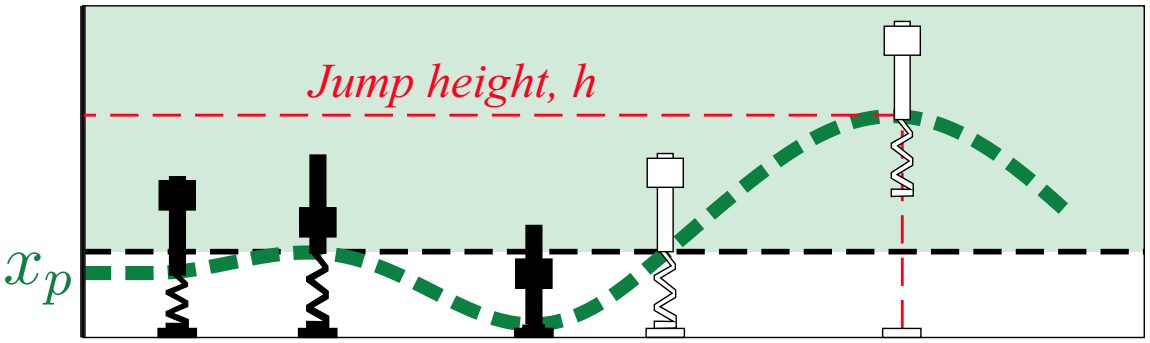

Figure 25: Jump height illustration.

To verify the theoretical model, we recreated the experiment in simulation with a MATLAB Simulink model that integrated Equation 1. MATLAB integrated the model with a 1000 x 1000 data point resolution, which had good agreement with experiment. We then used the model to generate other measures in the experiment such as number of jumps to execute the final jump, lift-off time, and internal deformation power, P_{def}, which is defined as the power generated by internal forces required to

control x_a excluding external forces such as gravity and spring forces. In general, the power output of a body can be expressed as the product of its velocity and force exerted $P = \dot{x}F$. In the case of the robot, power contributions of both the thrust rod and actuator must be considered individually, $P = \dot{x}_p F_p + \dot{x}_A F_a$, where the absolute motor velocity is defined as $\dot{x}_A = \dot{x}_a + \dot{x}_p$. The internal deformation power is then expressed as $P_{def} = \dot{x}_p\big(F_p - \frac{m_p}{m}F_{ext}\big) + \dot{x}_A\big(F_a - \frac{m_a}{m}F_{ext}\big)$, where the external force is comprised of gravity and spring forces, $F_{ext} = -mg - \alpha\big(x_p k + \dot{x}_p c\big)$. The forces can be expressed in terms of mass and acceleration as $F_p = m_p\ddot{x}_p$, $F_a = m_a\ddot{x}_A$, and $F_{ext} = mA_{ext}$. The deformation power can then be simplified and expressed in terms of accelerations as

$$P_{def} = m_p\dot{x}_p(\ddot{x}_p - A_{ext}) + m_a\dot{x}_A(\ddot{x}_A - A_{ext}) \tag{2}$$

where the absolute motor acceleration is defined as $\ddot{x}_A = \ddot{x}_a + \ddot{x}_p$.

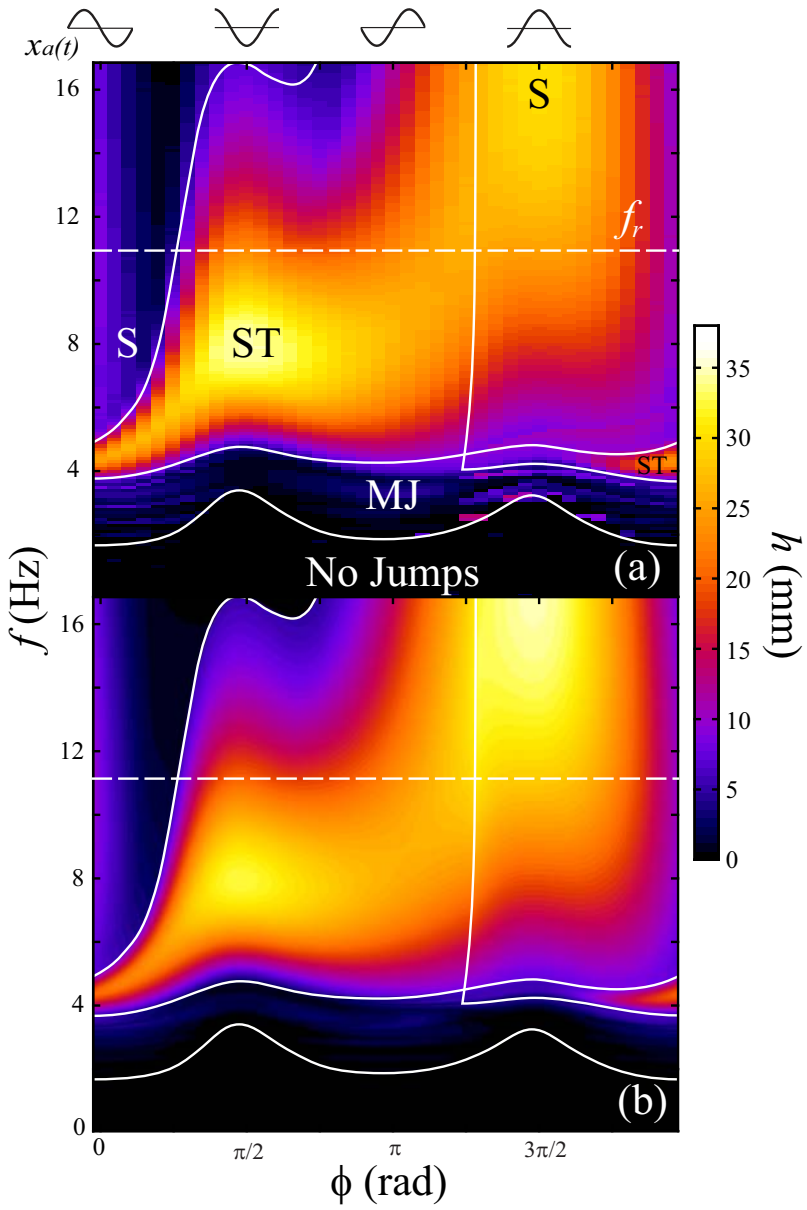

Figure 26: Jump height in the phase-frequency plane. (a) Experimental jump height, h, as a function of f and ϕ with illustrated actuator trajectories (top) at different ϕ with $A = 4$ mm. White lines (derived from model, see Figure 27) separate different jumping modes, with ST indicating stutter jump, S for single jump, and MJ for multi-jump. (b) Model simulation with the same parameters.

The model integration (Figure 26(b)) and experiment (Figure 26(a)) had excellent agreement. The data in each pixel of the experiment represents a jump height averaged over three trials. The variation from jump to jump was small, with the standard deviation being less than 0.5 mm, or approximately 1% of mean h, for frequencies higher than approximately 4 Hz. In a few phases, certain fractions of f_r below this 4 Hz exhibited significant variance due to small multi-jumps that occurred as a result of sub-resonant harmonics. This occurred in a fairly complex region in the $\phi - f$ plane labeled "MJ" for multi-jumps in Figure 26(a). These regions, delineated by white lines, were extracted from simulation (Figure 27). While this complex region is labeled multi-jumps, the model shows how this region periodically produced up to 5 small jumps while the motor is still oscillating, which is also evident in the experiment.

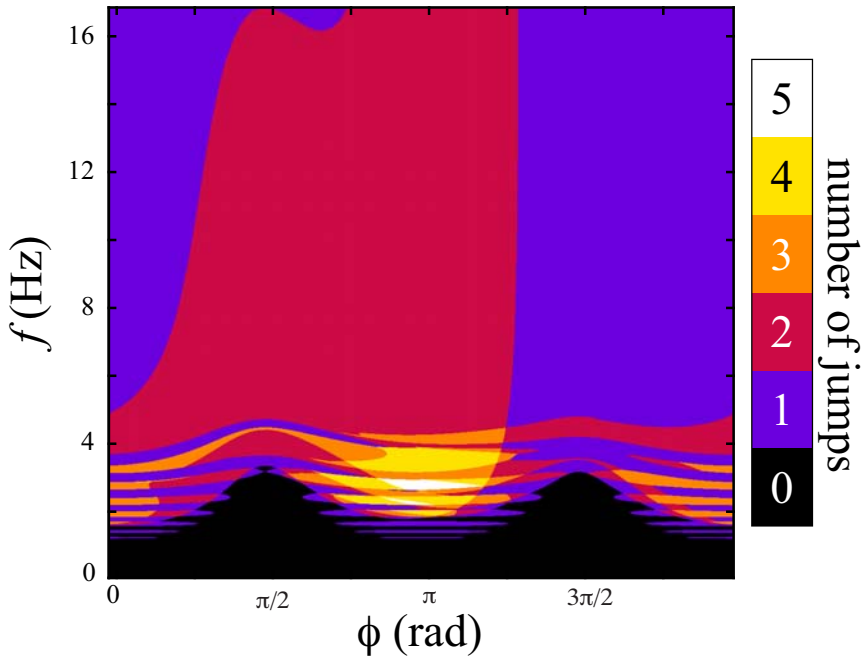

Figure 27: Number of jumps in the phase-frequency plane. Model simulation for number of jumps in the phase-frequency plane using experimental parameters. Single jumps are one jump, stutter jumps are two jumps.

For a fixed ϕ, above a critical frequency, f, the robot was able to lift off. Two broad maxima in h were observed, neither occurring at f_r, verifying our hypothesis derived from the minimum forcing amplitude experiment. The two local maxima correspond to two distinct modes of jumping: a "single jump" and a "stutter jump" (Figure 28). in the single jump mode, the robot compressed the spring and was propelled into the air. In the stutter jump mode, the robot performed a small initial jump followed by a larger second jump. For large ϕ, single jumps predominate, while stutter jumps occurred at lower f and ϕ.

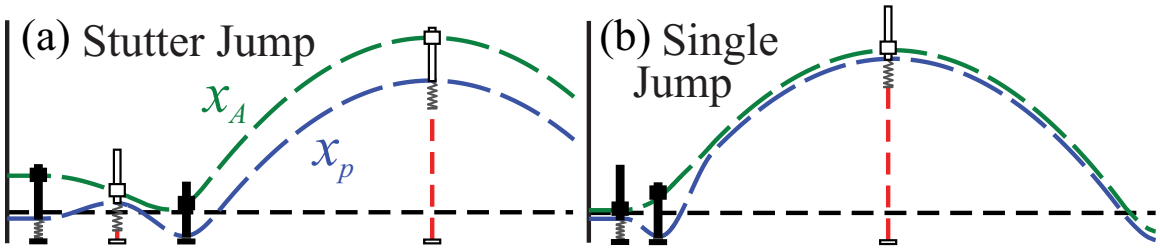

Figure 28: Jumping modes illustration. (a) Stutter jump. (b) Single jump. Robot is airborne (white robots) when the rod position, $x_p > 0$. Global actuator position, x_A, not to scale with rod length.

We also examined other characteristics associated with the maximum jump height for a given phase offset. At the optimal f of each phase, ϕ, the maximum h was determined and plotted versus phase which were insensitive to f and were nearly 10x larger than A (Figure 29(a)). The maximum h displayed two broad maxima which correspond to the two jumping modes previously mentioned, characterized by the optimal frequency and phase (Figure 29(b)). The stutter jump was optimal at $\phi = \pi/2$ radians, which is analogous to a countermovement, at $f < f_r$. And The single was optimal at $\phi = 3\pi/2$ radians, which is analogous to a squat jump, at $f > f_r$.

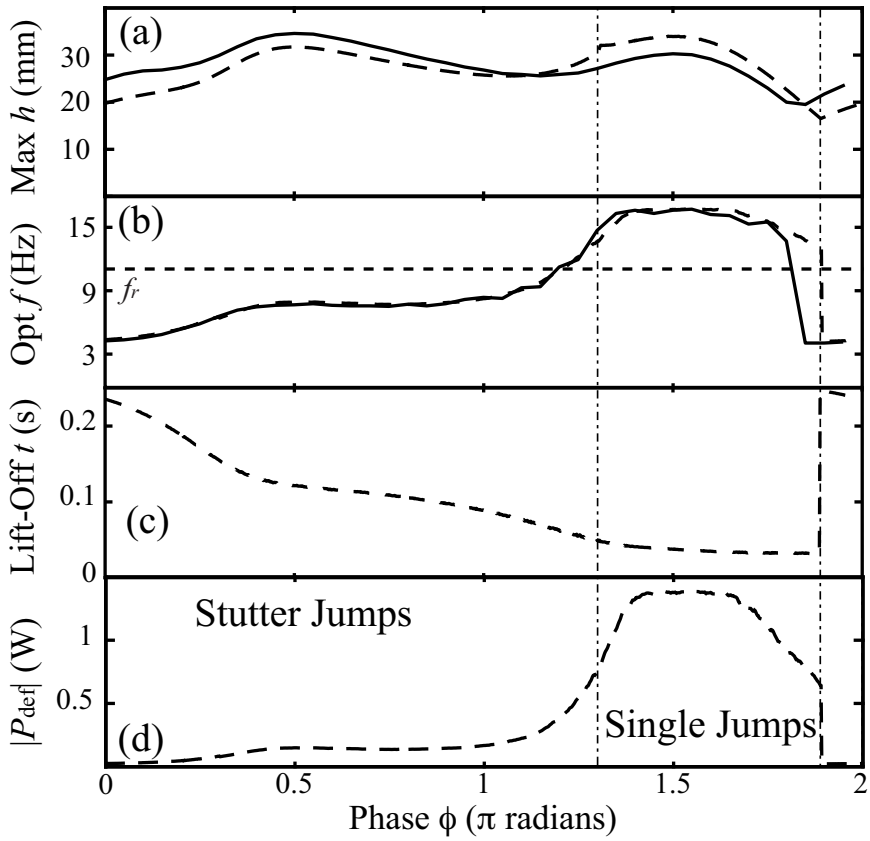

Figure 29: Comparison of various jump height results. Experimental (solid) and simulation (dashed) results of (a) maximum jump height at each phase, (b) the corresponding optimal frequency for each phase, (c) time to lift-off, and (d) deformation power at optimal frequency; initial transients are omitted in this calculation.

As will be shown in analysis, the peak power expended in deforming the system, P_{def}, scaled like f^3 and thus increased dramatically for single jumps (Figure 29(d)). So while the single jumps lift off faster than stutter jumps (Figure 29(c)), the single jumps also cost nearly an order of magnitude greater power than stutter jumps.

CHAPTER V

ANALYSIS

5.1 Theory of Transient Mixing

5.1.1 Minimum Pumping Amplitude

To understand why the optimal frequency to achieve lift-off is not f_0 during transient time-scale forcing ($N \leq 1$), we studied the equation for the thrust rod's trajectory, $x_p(t)$, by solving Equation 1 while on the ground ($\alpha = 1$). For our robot, the thrust rod's mass, m_p, is relatively small compared to the motor mass, m_a; thus, we made the assumption that $m_a = m$. Additionally, damping was also small, so we assumed no damping. Substituting $-A\omega^2 \sin(\omega t + \phi)$ for $\ddot{x}_a$ into Equation 1 and making the aforementioned assumptions, the equation of motion while on the ground becomes

$$\ddot{x}_p = A\omega^2 \sin(\omega t + \phi) - \omega_0^2 x_p - g \tag{3}$$

where the natural frequency, $\omega_0 = \sqrt{k/m}$. To simplify equations, the units of frequency in the following derivations are radians/second, $\omega = 2\pi f$, and $\omega_0 = 2\pi f_0$. Solving the differential equation, Equation 3, the rod's trajectory equation is

$$x_p(t) = \frac{A\omega^2}{\omega_0^2 - \omega^2} \sin(\omega t + \phi) + C_1 \cos(\omega_0 t) + C_2 \sin(\omega_0 t) - \frac{g}{\omega_0^2} \tag{4}$$

Deriving Equation 4, the rod's velocity is

$$\dot{x}_p(t) = \frac{A\omega^3}{\omega_0^2 - \omega^2} \cos(\omega t + \phi) - \omega_0 C_1 \sin(\omega_0 t) + \omega_0 C_2 \cos(\omega_0 t) \tag{5}$$

Starting from rest at the equilibrium position, the initial conditions are $x_p(0) = -\frac{g}{\omega_0^2}$ and $\dot{x}_p(0) = 0$. Using these initial conditions, we then solve for C_1 and C_2.

$$C_1 = -\sin(\phi) \frac{A\omega^2}{\omega_0^2 - \omega^2} \tag{6}$$

$$C_2 = -\cos(\phi)\frac{A\omega^2}{\omega_0^2 - \omega^2}\frac{\omega}{\omega_0} \tag{7}$$

Substituting Equations 6 and 7 into Equation 4, the trajectory equation becomes

$$x_p(t) = \frac{A\omega^2}{\omega_0^2 - \omega^2}\left(\sin(\omega t + \phi) - \sin(\phi)\cos(\omega_0 t) - \frac{\omega}{\omega_0}\cos(\phi)\sin(\omega_0 t)\right) - \frac{g}{\omega_0^2} \tag{8}$$

Considering a phase offset of $\pi/2$, Equation 8 simplifies to

$$x_p(t) = \frac{A\omega^2}{\omega_0^2 - \omega^2}\big(\cos(\omega t) - \cos(\omega_0 t)\big) - \frac{g}{\omega_0^2} \tag{9}$$

The robot's position is thus a prefactor times the sum of two competing sinusoids (one at the natural frequency, ω_0, and the other at the forcing frequency, ω). While the prefactor increases the magnitude of the oscillatory response for ω near ω_0, the competing sinusoids introduce destructive interference that suppresses the amplification of the oscillation magnitude when ω is too close to ω_0. Moving off resonance, the prefactor favors higher ω over lower. A local minimum also occurs in the minimum forcing amplitude vs. frequency data for $\phi = \pi/2$ (Figure 23) due to the local maximization of total mechanical energy (potential elastic energy and kinetic energy) at the end of one cycle of motor forcing, ($t = 2\pi/\omega$). Thus, during transient time scales, the oscillation of the rod was not given sufficient time to amplify in magnitude, making resonant amplification less of a factor in determining optimal frequency than the combination of resonant amplification and destructive interference from transient sinusoidal mixing.

5.1.2 Maximum Jump Height

While at first glance, Equation 1 looks completely tractable, it was only because the robot was always on the ground before the first lift-off that we were able to analytically derive the trajectory equation for our discussion on minimum pumping amplitude. The discontinuity associated with the factor α renders the equation piecewise linear, or nonlinear. However, an analytical argument similar to the argument made for

minimum pumping amplitude can be made to explain why the optimal frequency for jump height during single jumps is greater than the natural frequency, since, during single jumps, $\alpha = 1$ until final take-off.

Consider first the peak labeled S in Figure 26(a), representing the highest single jumps. This peak occurred at actuator phases near $\phi = 3\pi/2$. For a relatively slow thrust rod mass, jump height was proportional to the square of the absolute motor velocity, $\dot{x}_A(t) = \dot{x}_p + \dot{x}_a$, at take-off, where $\dot{x}_a(t) = A\omega\cos(\omega t + \phi)$. Using the same assumptions made for minimum forcing amplitude the absolute motor velocity can be solved by adding $\dot{x}_a(t)$ and $\dot{x}_p(t)$ from Equation 5 for $\phi = 3\pi/2$.

$$\dot{x}_p(t) = \frac{A\omega^2}{\omega_0^2 - \omega^2}\omega_0\left(\frac{\omega_0}{\omega}\sin(\omega t) - \sin(\omega_0 t)\right) \tag{10}$$

Like in Equation 9, $\dot{x}_A(t)$ is also a prefactor times the sum of two opposing sinusoids. The same arguments of transient mixing can thus be made to describe the take-off velocity of the robot, which will be optimized at a frequency, $\omega > \omega_0$, or $f > f_0$. Additionally, while the prefactor favors a higher f over frequencies lower than f_0, the optimal frequency is also upper-bounded, since a higher f produces a faster time to take-off, which limits the time available to amplify power.

5.2 The Stutter Jump

5.2.1 A Conceptual Understanding

Understanding the presence and optimality of the stutter jump is more complicated than the single jump, since the existence of two jumps introduces nonlinearities due to the piece-wise nature of Equation 1, making it difficult to dissect analytically. However the unexpected emergence of the stutter jump can be understood through a conceptual analysis. Consider, for example, the case of $\phi = \pi/2$, so that the initial actuator acceleration is negative. This causes the less massive thrust rod to be accelerated upward before moving down to compress the spring and the lift off again.

Interestingly, the stutter jump was observed for phases somewhat larger than π (Figure 26(a)), in which the initial actuator acceleration is expected to progress positively from 0. This phenomenon can be explained by the actuator's physical constraint. Regardless of phase offset, the actuator must start from rest. Any phase offset corresponding to a non-zero initial actuator velocity causes an initial impulse acceleration to the intended initial velocity. This results in an initial actuator trajectory that is not an ideal sine wave. For a phase such as $\phi = \pi$, the initial relative actuator acceleration is large and negative (Figure 30), which briefly causes a large upward acceleration in the rod, causing an intermediate hop.

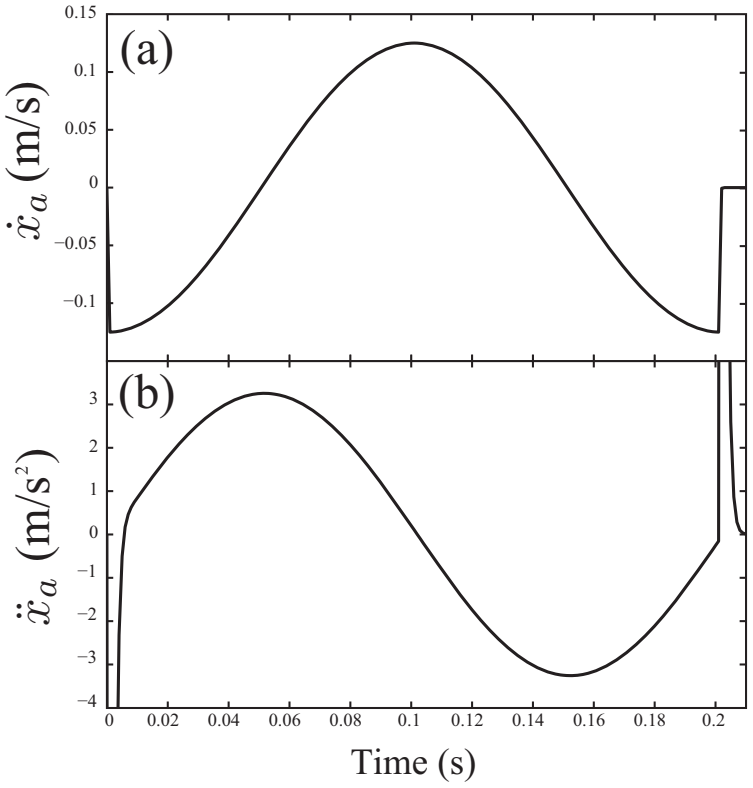

Figure 30: Simulation of an initial actuator impulse. $\phi = \pi$.

5.2.2 Optimization

The key to understanding the optimization of the stutter jump is to consider the system energetics and the conditions that maximize the total work done during the

forcing cycle. The instantaneous power input is $P = F_{ext} v_m$, where the F_{ext} is the total external force, which includes gravity and spring forces, and v_m is the velocity of the center of mass of the robot, which can be approximated as $\dot{x}_A$, since $m_p << m_a$. The total work done be external forces is maximized when $\dot{x}_A$ both is large in magnitude and has the same sign as F_{ext}.

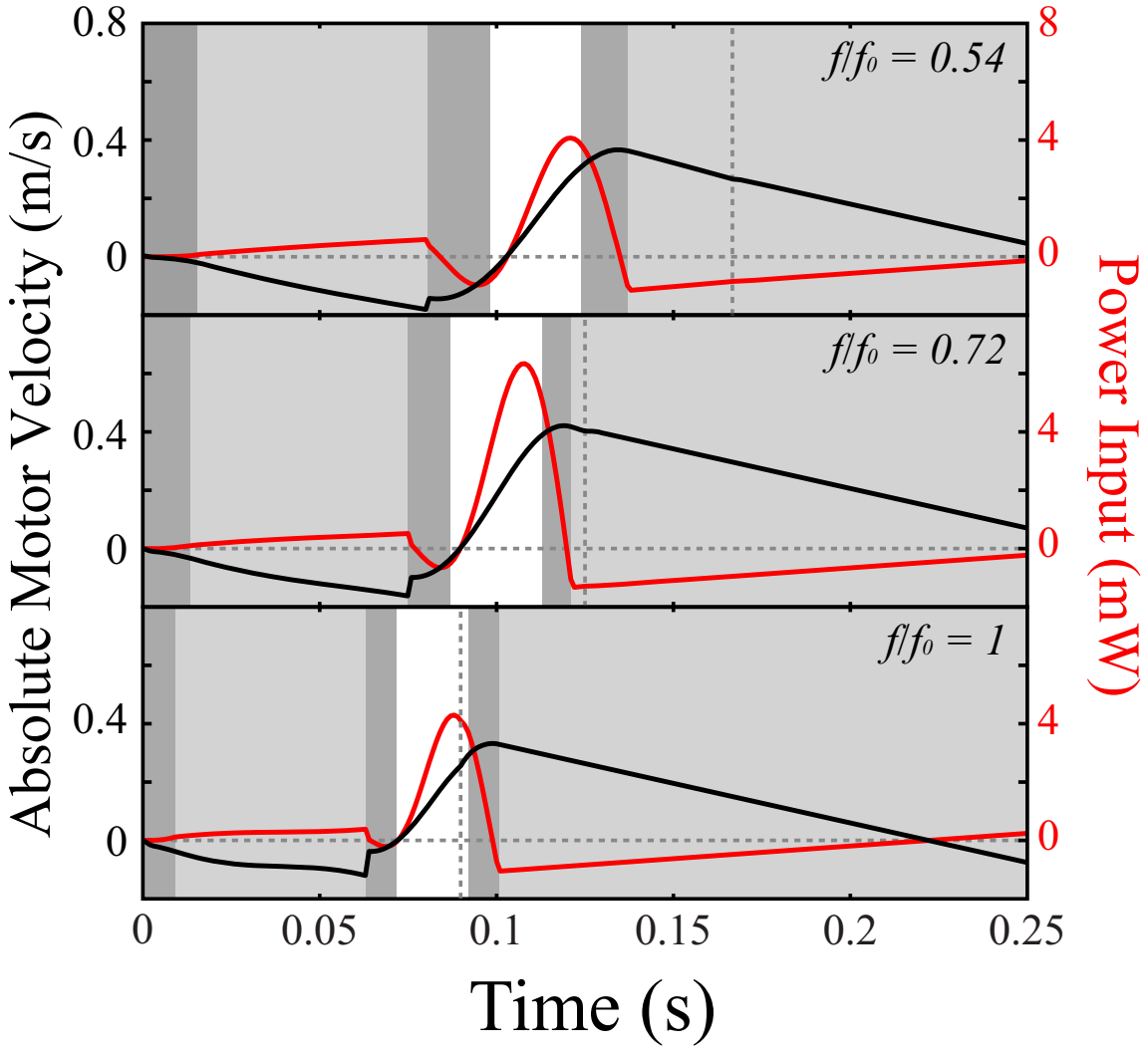

Figure 31: Simulated input power and motor velocity at different f. Absolute actuator velocity (black) and power input by external forces (red) for $f/f_0 = 0.54$, 0.72 (optimal) and 1, at $\phi = \pi/2$. The vertical dotted line indicates the time past which $\dot{x}_a = 0$. Light grey areas indicate the aerial state ($x_p > 0$); dark grey indicates negative force ground state ($mg/k < x_p <\leq 0$); white represents positive force ground state ($x_p \leq (mg/k)$).

Figure 31 illustrates this situation for $\phi = \pi/2$, which is when the stutter jump is optimal. At $f = f_0$ (lower panel), the actuation is too fast and the actuator turns off well before lift-off. At a low f (top panel), the actuation is too slow, causing the

actuator to stop well after lift-off. This results in much of the power stroke being wasted in the air. The optimal driving frequency (middle panel) lies somewhere in between the previous two frequencies, in which the motor is forced until lift-off occurs, maximizing the proportion of the stroke that benefits from elastic power amplification while on the ground.

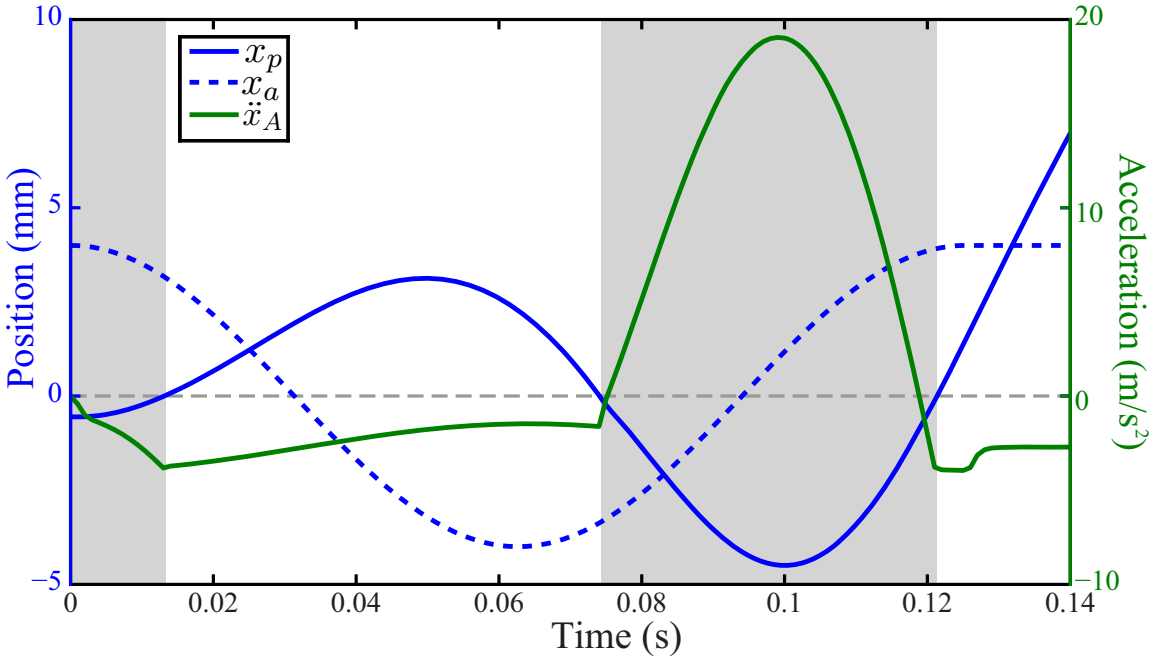

Figure 32: Simulated trajectory of the optimal stutter jump. $\phi = \pi/2$, $f = 7.98$ Hz. Grey areas indicated the grounded state; white areas indicate the aerial state.

Figure 32 illustrates the trajectory of this optimal frequency. The motor starts at the top and moves down then back up relative to the rod (countermovement). Just milliseconds before making contact with the ground, the motor begins to move upward along the rod, pushing the rod down into the ground. Interestingly, the subtlety of pre-landing motor movement has been observed to benefit human jumping during drop jumps [58]. Once on the ground, the spring is eventually compressed maximally due to a combination of momentum from falling and motor forcing. When the spring reaches maximum compression, both $\dot{x}_a$ and $\ddot{x}_A$ are at maximal values. The combination of

these two maximizations causes optimal power amplification of the motor stroke and an explosive acceleration during push-off, maximizing $\dot{x}_A$ at lift-off.

Thus the optimality of the stutter jump not only depends on the phasing of competing sinusoids while on the ground, but also on the proper timing of aerial and ground states. The later does not generally occur at f_0. The frequency bandwidth in which stutter jumps are optimal is more narrow than for single jumps, which can be explain by the additional sensitivity to proper timing. Another consequence is a strong dependence of optimal f with respect to the forcing amplitude, A. A larger A produces lower optimal f, and a smaller A results in a higher optimal f. This strong amplitude dependence is in direct contrast to the single jump mode, which does not show a strong dependence to A.

5.2.3 Deformation Power Comparison

The stutter jump uses downward momentum to assist in spring compression, which allows an optimal stutter jump to achieve comparable jump height to an optimal single jump while the motor oscillates at a lower f. Consequently, the stutter jump also uses nearly an order of magnitude less deformation power than the single jump, which can be linked directly to the forcing frequency, f. The rod acceleration, $\ddot{x}_p$, and the absolute motor acceleration, $\ddot{x}_A$, can be expressed as the following equations:

$$\ddot{x}_p = A\omega^2 \frac{m_a}{m} \sin(\omega t + \phi) + A_{ext} \tag{11}$$

$$\ddot{x}_A = -A\omega^2 \frac{m_p}{m} \sin(\omega t + \phi) + A_{ext} \tag{12}$$

where A_{ext} is the sum the external force accelerations as defined in Section 4.1. Substituting Equations 11 and 12 into Equation 2, the deformation power becomes

$$P_{def} = m_p \dot{x}_p \left(A\omega^2 \frac{m_a}{m} \sin(\omega t + \phi) \right) + m_a \big(\dot{x}_p + A\omega \cos(\omega t + \phi) \big) \left(-A\omega^2 \frac{m_p}{m} \sin(\omega t + \phi) \right) \tag{13}$$

which simplifies to

$$P_{def} = -A^2 f^3 \frac{m_a m_p}{m} \cos(\omega t + \phi) \sin(\omega t + \phi) \tag{14}$$

such that the maximum deformation power is expressed as $P_{def,max} = \frac{m_a m_p}{2m} A^2 f^3$. Thus, internal deformation power is proportional to the cube of the forcing frequency. While the simple jump is quicker, which is beneficial when a fast escape is essential, the stutter jump is optimal at a lower frequency and thus requires less internal power to produce.

CHAPTER VI

CONCLUSION

6.1 Accomplishments

In this thesis, we combined experiment and simulation to analyze a simple jumping robot based on the 1D SLIP model to uncover fundamental principles of maximal height jumping. We found the performance of the robot to be quite rich and highly sensitive to the starting phase offset, largely a result of the transient dynamics of the system. Oscillating the motor for more than 1 cycle while on the ground allowed the use of small amplitudes at f_0 to achieve lift-off. However, since the objective of jumping was not lift-off alone but also jump height, the time spent on the ground was less than 1 cycle, resulting in the transient dynamics of the robot to produce non-resonant optimal frequencies for jump height.

For certain sinusoidal parameters, the robot becomes a hybrid piecewise linear system as a stutter jump emerges. Analysis of a simplified model revealed that impulse accelerations and discontinuous transitions to the aerial state were essential ingredients in understanding the emergence and dynamics of the stutter jump. The mode achieved comparable jump height to single jumps but required less power. This result has powerful implications with respect to the energetic benefits of performing such a jump, since hopping robots based on the SLIP model can directly benefit from this result in performing maximal height jumps, and more sophisticated multi-link robots may also find guidance from these results.

Biologically, our model is in accord with a previous model of maximal height bipedal jumping which predicted that a countermovement could achieve a greater jump height than a squat jump [5]. In our study, the single jump, which is produced

with a squat jump maneuver, must be performed faster to achieve the jump height of the slower stutter jump, which is produced with a countermovement. Preparatory hops have been observed in various primates [47][109][36] and rodents [63][41]. Humans regularly perform stutter jumps during certain volleyball techniques [35]. Based on the power arguments made in this thesis, we hypothesize that this mode is advantageous for various animals.

6.2 Future directions

The emergence of interesting answers lead to more interesting questions. Below are some possible directions that our work may take, most being natural extensions of this research, and one being a completely different paradigm with which to approach this research.

6.2.1 Model comparison

A systematic comparison of this model with biological hoppers would be beneficial. While the results of the experiments presented in this thesis are specific to the parameters of the robot used, jump height results are consistent for given value of mg/kA. In other words, if mg/kA, or $x_{p,equilibrium}/A$, remains the same, jump height relative to amplitude, h/A, remains the same when plotted as a color map in the $f - \phi$ plane as in Figure 33.

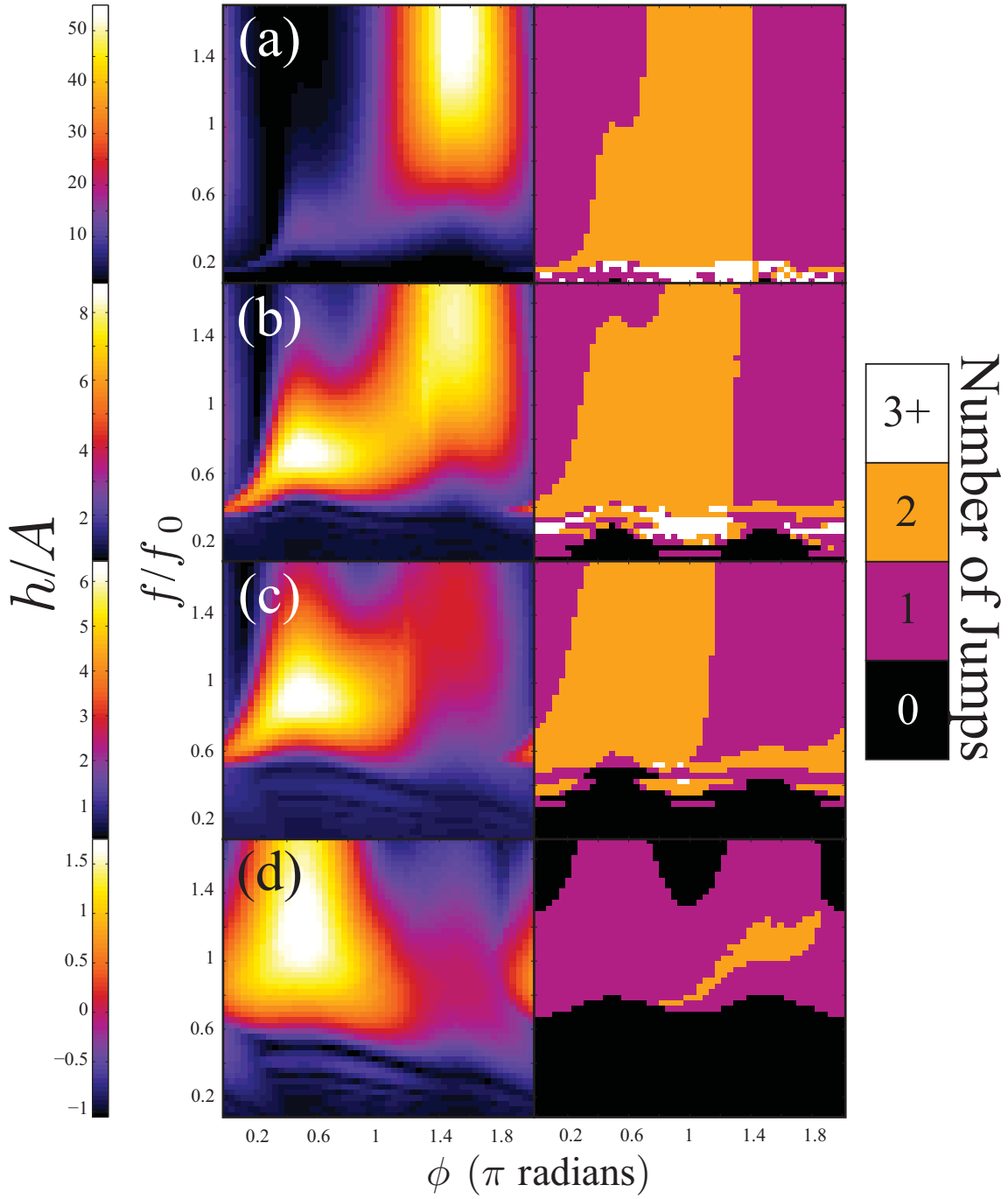

Figure 33: Jump heights for different values of mg/kA. Simulation data for $mg/kA =$ (a) 0.02, (b) 0.14 (robot parameters), (c) 0.4, and (d) 2. Left panel shows jump height color map, right panel shows number of jumps.

It would be interesting to experimentally measure k for different animals and determine the jumping modes that are theoretically advantageous according to mg/kA. In concert with theoretical predictions, experimental observations of the preferred jumping modes for maximal height jumping can also be performed. Humans can be our first test species, as we can compare the performance of different jumping modes. A potential intermediary step in comparing with biology would be to recreate the jump height experiment presented in this thesis using a simulation of Alexander's model [5], which is a more anatomically accurate model of biological bipedal jumping than a one dimensional SLIP model.

6.2.2 Non-sinusoidal forcing

In our research, we used a sine wave to model common forcing strategies for jumping, such as the squat jump and countermovement. Such a function also allowed us to sweep different parameters and quantitatively characterize movement strategies. However, real animals do not move in perfect sine waves to produce jumps. It would be interesting to see how jump performance is affected by using different shaped trajectories. For example, the final push-off phase of a stutter jump might benefit from a forcing frequency that is faster than the frequency necessary up to maximal compression.

6.2.3 Traversing an obstacle course

We have uncovered the requirements for ϕ and f to achieve maximum jump height at a given A when jumping from rest. Yet, we have not considered the sinusoidal parameter requirements for specific height control or control of lift-off time given a non-zero initial velocity. Such requirements would be essential to know for a hopping robot to traverse diverse terrain with varying obstacle sizes. We can consider mapping an input velocity to an output velocity and lift-off time given a particular set of (A, f, ϕ).

6.2.4 Introducing environmental complexity

The results presented in this thesis describe the optimal movements of a simple robot interacting with a simple environment, namely, 1D motion over hard ground. At what point are added complexities to our model beneficial, necessary or possibly detrimental? What types of model complexities complement given environmental complexities? As described in the introduction, many researchers have addressed the complexities necessary for hopping and jumping robots to achieve balance in 2D and 3D environments. But little work has been done on the complexities required to achieve optimal jumping on deformable surfaces. For compliant surfaces such as branches or trampolines, it may be as simple as changing the movement strategy. However, jumping on granular media such as sand can result in much more complex interactions, requiring more complex solutions for increased jumping performance. For example, choosing the right movement strategy in addition to a foot may provide increased performance. A foot can vary in surface area, shape, compliance and actuation.

6.2.5 An interactive "crowd-sourcing" approach

One fascinating aspect of biological locomotion is that, whether by instinct or learning, the movement strategies that are optimal for a given task are chosen naturally. In humans, this innate familiarity with one's body translates to typing, texting and playing video games. As such, an interactive simulation of our robot may provide some striking insight into optimal modes of movement for different jumping tasks without having to perform brute force sweeps of a parameter space. This approach would complement a study in non-sinusoidal movements for jumping and traversing an obstacle course. The model is sufficiently simple to simulate in real-time as a web based game or a mobile phone game. Given a specific challenge, players that get

the highest scores would upload time domain simulation data such as forces, velocities and positions to our servers for analysis. Given accepted force law models, such a crowd-sourcing approach could also complement a study on jumping in granular media.

REFERENCES

[1] Aerts, P., "Vertical jumping in Galago senegalensis: the quest for an obligate mechanical power amplifier," *Transactions of the Royal Society*, vol. 353, no. 1375, pp. 1607–1620, 1998.

[2] Ahmadi, M. and Buehler, M., "The ARL monopod II running robot: Control and energetics," in *Robotics and Automation, 1999. Proceedings. 1999 IEEE International Conference on*, vol. 3, pp. 1689–1694, 1999.

[3] Akinfiev, T., Armada, M., and Montes, H., "Vertical movement of resonance hopping robot with electric drive and simple control system," *IEEE 11th Mediterranean Conference on Control and Automation (MED03), Greece*, 2003.

[4] Albro, J. and Bobrow, J., "Optimal motion primitives for a 5 dof experimental hopper," in *Robotics and Automation, 2001. Proceedings 2001 ICRA. IEEE International Conference on*, vol. 4, pp. 3630–3635, 2001.

[5] Alexander, R. M., "Leg design and jumping technique for humans, other vertebrates and insects.," *Philosophical transactions of the Royal Society of London. Series B, Biological sciences*, vol. 347, pp. 235–48, Feb. 1995.

[6] Alexander, R. M., "Modelling approaches in biomechanics.," *Philosophical transactions of the Royal Society of London. Series B, Biological sciences*, vol. 358, pp. 1429–35, Sept. 2003.

[7] Alexander, R. M. and Vernon, A., "The mechanics of hopping by kangaroos (Macropodidae)," *Journal of Zoology*, vol. 177, pp. 265–303, Aug. 1973.

[8] Alexander, R. M., "Tendon elasticity and muscle function.," *Comparative biochemistry and physiology. Part A, Molecular & integrative physiology*, vol. 133, pp. 1001–11, Dec. 2002.

[9] Alexander, R., "Elastic mechanisms in primate locomotion," *Zeitschrift für Morphologie und Anthropologie*, 1991.

[10] Alexander, R., *Principles of animal locomotion*. Princeton University Press, 2002.

[11] Alexander, R. M., "Optimum take-off techniques for high and long jumps.," *Philosophical transactions of the Royal Society of London. Series B, Biological sciences*, vol. 329, pp. 3–10, July 1990.

[12] Allison, J., "Monopod Jumping Robot," 2002.

[13] Armour, R., Paskins, K., Bowyer, A., Vincent, J., Megill, W., and Bomphrey, R., "Jumping robots: a biomimetic solution to locomotion across rough terrain.," *Bioinspiration & biomimetics*, vol. 2, pp. S65–82, Sept. 2007.

[14] Babic, J., "Biarticular Legged Robot : Design and Experiments," in *2008 IEEE International Conference on Robotics and Biomimetics*, pp. 155–159, 2009.

[15] Beatty, M. F., *Principles of engineering mechanics*. Plenium Press, 1986.

[16] Bennet-Clark, H. C., "The energetics of the jump of the locust Schistocerca gregaria.," *The Journal of experimental biology*, vol. 63, pp. 53–83, Aug. 1975.

[17] Bennet-Clark, H. C. and Lucey, E. C., "The jump of the flea: a study of the energetics and a model of the mechanism.," *The Journal of experimental biology*, vol. 47, pp. 59–67, Aug. 1967.

[18] Bennet-Clark, H., "Energy storage in jumping animals," *Perspectives in Experimental Biology*, 1976.

[19] Bennet-Clark, H., "Scale effects in jumping animals," *Scale effects in animal locomotion*, pp. 185–201, 1977.

[20] Bennett, M., Ker, R., Imery, N., and Alexander, R., "Mechanical properties of various mammalian tendons," *Journal of Zoology*, vol. 209, no. 4, pp. 537–548, 1986.

[21] Berkemeier, M. and Desai, K., "Control of hopping height in legged robots using a neural-mechanical approach," in *Robotics and Automation, 1999. Proceedings. 1999 IEEE International Conference on*, pp. 1695–1701, 1999.

[22] Biewener, A., Alexander, R. M., and Heglund, N. C., "Elastic energy storage in the hopping of kangaroo rats (Dipodomys spectabilis)," *Journal of Zoology*, vol. 195, pp. 369–383, Aug. 1981.

[23] Biewener, A., Konieczynski, D., and Baudinette, R., "In vivo muscle force-length behavior during steady-speed hopping in tammar wallabies.," *The Journal of experimental biology*, vol. 201, pp. 1681–94, June 1998.

[24] Blickhan, R., "The spring-mass model for running and hopping," *Journal of biomechanics*, vol. 22, no. 11, pp. 1217–1227, 1989.

[25] Blickhan, R. and Full, R., "Similarity in multilegged locomotion: Bouncing like a monopode," *Journal of Comparative Physiology A: Neuroethology ...*, 1993.

[26] Blickhan, R., Seyfarth, A., Geyer, H., Grimmer, S., Wagner, H., and Günther, M., "Intelligence by mechanics.," *Philosophical transactions. Series A, Mathematical, physical, and engineering sciences*, vol. 365, pp. 199–220, Jan. 2007.

[27] Bobbert, M., "Dependence of human squat jump performance on the series elastic compliance of the triceps surae: a simulation study," *Journal of Experimental Biology*, 2001.

[28] Bobbert, M., Mackay, M., Schinkelshoek, D., Huijing, P., and van Ingen Schenau, G., "Biomechanical analysis of drop and countermovement jumps," *European journal of applied physiology and occupational physiology*, vol. 54, pp. 566–573, 1986.

[29] Brackenbury, J. and Wang, R., "Ballistics and visual targeting in flea-beetles (Alticinae)," *The Journal of Experimental Biology*, vol. 198, pp. 1931–42, Jan. 1995.

[30] Brown, B. and Zeglin, G., "The bow leg hopping robot," *Robotics and Automation*, 1998.

[31] Cavagna, G., Thys, H., and Zamboni, A., "The sources of external work in level walking and running.," *The Journal of physiology*, vol. 262, no. 3, pp. 639–657, 1976.

[32] Cham, J. and Cutkosky, M., "Dynamic stability of open-loop hopping," *Journal of dynamic systems, measurement, and control*, vol. 129, no. 3, p. 275, 2007.

[33] Choi, I. and Park, K., "Variations in take-off velocity of anuran amphibians: relation to morphology, muscle contractile function and enzyme activity," *Comparative Biochemistry and Physiology Part A: Physiology*, vol. 113, no. 4, pp. 393–400, 1996.

[34] Choi, I., Shim, J. H., and Ricklefs, R. E., "Morphometric relationships of take-off speed in anuran amphibians.," *Journal of experimental zoology. Part A, Comparative experimental biology*, vol. 299, pp. 99–102, Oct. 2003.

[35] Coutts, K., "Kinetic differences of two volleyball jumping techniques," *Medicine & Science in Sports & Exercise*, 1982.

[36] Demes, B., Jungers, W., Fleagle, J., Wunderlich, R., Richmond, B., and Lemelin, P., "Body size and leaping kinematics in Malagasy vertical clingers and leapers," *Journal of Human Evolution*, vol. 31, pp. 367–388, Oct. 1996.

[37] Demes, B., Jungers, W., Gross, T., and Fleagle, J., "Kinetics of Leaping Primates: Influence of Substrate Orientation and Compliance," *American Journal of Physical Anthropology*, vol. 96, no. 4, pp. 419–429, 1995.

[38] Dickinson, M. H., Farley, C., Full, R., Koehl, M., Kram, R., and Lehman, S., "How Animals Move: An Integrative View," *Science*, vol. 288, pp. 100–106, Apr. 2000.

[39] Emerson, S., "Allometry and Jumping in Frogs : Helping the Twain meet," *Evolution*, vol. 32, no. 3, pp. 551–564, 1978.

[40] Emerson, S., "Jumping and leaping," *Functional vertebrate morphology*, 1985.

[41] Essner, R. L., "Three-dimensional launch kinematics in leaping, parachuting and gliding squirrels.," *The Journal of experimental biology*, vol. 205, pp. 2469–77, Aug. 2002.

[42] Evans, M. E. G., "The jump of the click beetle (Coleoptera, Elateridae)-a preliminary study," *Journal of Zoology*, vol. 167, pp. 319–336, Aug. 1972.

[43] Full, R. J. and Koditschek, D. E., "Templates and anchors: neuromechanical hypotheses of legged locomotion on land.," *The Journal of experimental biology*, vol. 202, pp. 3325–32, Dec. 1999.

[44] Galantis, A. and Woledge, R., "The theoretical limits to the power output of a muscletendon complex with inertial and gravitational loads," *Proceedings of the Royal Society of London. Series B: Biological Sciences*, vol. 207, no. 1523, pp. 1493–1498, 2003.

[45] German, J., "Hop to it: Sandia hoppers leapfrog conventional wisdom about robot mobility," *Sandia Lab News*, vol. 52, no. 21, 2000.

[46] Gray, J., *How animals move*. 1953.

[47] Günther, M., "Biomechanical prerequisites for the leap-off of Senegal galagos.," *Zeitschrift für Morphologie und Anthropologie*, 1985.

[48] Günther, M., Ishida, H., Kumakura, H., and Nakano, Y., "The jump as a fast mode of locomotion in arboreal and terrestrial biotopes," *Zeitschrift für Morphologie und Anthropologie*, vol. 78, no. 3, pp. 341–372, 1991.

[49] Hale, E., Schara, N., Burdick, J., and Fiorini, P., "A minimally actuated hopping rover for exploration of celestial bodies," in *Robotics and Automation, 2000. Proceedings. ICRA'00. IEEE International Conference on*, vol. 1, pp. 420–427, Ieee, 2000.

[50] Hall-Craggs, E. C., "an Osteometric Study of the Hind Limb of the Galagidae.," *Journal of anatomy*, vol. 99, pp. 119–26, Jan. 1965.

[51] Harris, M. a. and Steudel, K., "The relationship between maximum jumping performance and hind limb morphology/physiology in domestic cats (Felis silvestris catus).," *The Journal of experimental biology*, vol. 205, pp. 3877–89, Dec. 2002.

[52] Hatze, H., "A comprehensive model for human motion simulation and its application to the take-off phase of the long jump," *Journal of Biomechanics*, vol. 14, no. 3, pp. 135–142, 1981.

[53] Hayashi, R. and Tsujio, S., "High-performance jumping movements by pendulum-type jumping machines," in *Intelligent Robots and Systems, 2001. Proceedings. 2001 IEEE/RSJ International Conference on*, pp. 722–727, 2001.

[54] Heitler, W., "The locust jump. Specialisations of the metathoracic femoral-tibial joint," *J. comp. Physiol*, 1974.

[55] Hill, A., "The heat of shortening and the dynamic constants of muscle," *Proceedings of the Royal Society of London. Series B, Biological Sciences*, vol. 126, no. 843, pp. 136–195, 1938.

[56] Hill, A., "The dimensions of animals and their muscular dynamics," 1949.

[57] Hof, A., "In vivo measurement of the series elasticity release curve of human triceps surae muscle," *Journal of biomechanics*, vol. 31, pp. 793–800, Sept. 1998.

[58] Horita, T., Komi, P. V., Nicol, C., and Kyröläinen, H., "Interaction between pre-landing activities and stiffness regulation of the knee joint musculoskeletal system in the drop jump: implications to performance.," *European journal of applied physiology*, vol. 88, pp. 76–84, Nov. 2002.

[59] Hubbard, M. and Trinkle, J., "Clearing maximum height with constrained kinetic energy," *Journal of applied mechanics*, vol. 52, no. 1, pp. 179–184, 1985.

[60] Hyon, S. H. and Mita, T., "Development of a Biologically Inspired Hopping Robot "Kenken"," in *International Conference on Robotics and Automation*, no. May, pp. 3984–3991, 2002.

[61] James, R. S., Navas, C. a., and Herrel, A., "How important are skeletal muscle mechanics in setting limits on jumping performance?," *The Journal of experimental biology*, vol. 210, pp. 923–33, Mar. 2007.

[62] James, R., Wilson, R., de Carvalho, J., Kohlsdorf, T., Gomes, F., and Navas, C., "Interindividual differences in leg muscle mass and pyruvate kinase activity correlate with interindividual differences in jumping performance of hyla multilineata," *Physiological and Biochemical Zoology*, vol. 78, no. 5, pp. 857–867, 2005.

[63] Keith, M., Scheibe, J., and Hendershott, A., "Launch dynamics in Glaucomys volans," *Biology of gliding mammals*, 2000.

[64] Ker, R., Dimery, N., and Alexander, R., "The role of tendon elasticity in hopping in a wallaby (Macropus rufogriseus)," *Journal of Zoology*, 1986.

[65] Kikuchi, F., Ota, Y., and Hirose, S., "Basic performance experiments for jumping quadruped," in *Intelligent Robots and Systems, 2003.(IROS 2003). Proceedings. 2003 IEEE/RSJ International Conference on*, 2003.

[66] Koditschek, D. and Bühler, M., "Analysis of a simplified hopping robot," *The International Journal of Robotics Research*, vol. 10, no. 6, pp. 587–605, 1991.

[67] Komi, P. and Bosco, C., "Utilization of stored elastic energy in leg extensor muscles by men and women.," *Medicine and Science in Sports*, 1978.

[68] Kovac, M., Fuchs, M., Guignard, A., Zufferey, J., and Floreano, D., "A miniature 7g jumping robot," in *ICRA 2008. IEEE International Conference on Robotics and Automation*, no. figure 3, pp. 373–378, IEEE, 2008.

[69] Kubo, K., Kawakami, Y., Fukunaga, T., James, R. S., Navas, C. A., and Herrel, A., "Influence of elastic properties of tendon structures on jump performance in humans," *Journal of Applied Physiology*, no. 87, pp. 2090–2096, 1999.

[70] Leavitt, J., Bobrow, J., and Sideris, A., "Robust balance control of a one-legged, pneumatically-actuated, acrobot-like hopping robot," in *Robotics and Automation, 2004. Proceedings. ICRA'04. 2004 IEEE International Conference on*, 2004.

[71] Lee, W. and Raibert, M., "Control of hoof rolling in an articulated leg," in *Proceedings. 1991 IEEE International Conference on Robotics and Automation*, pp. 1386–1391, IEEE Comput. Soc. Press, 1991.

[72] Li, C. and Umbanhowar, P., "Sensitive dependence of the motion of a legged robot on granular media," *Proceedings of the*, vol. 106, no. 9, pp. 3029–3034, 2009.

[73] Losos, J., "The evolution of form and function: morphology and locomotor performance in West Indian Anolis lizards," *Evolution*, 1990.

[74] Losos, J., Papenfuss, T., and Macey, J., "Correlates of sprinting, jumping and parachuting performance in the butterfly lizard, Leiolepis belliani," *Journal of Zoology*, 1989.

[75] Lutz, G. J. and Rome, L. C., "Built for jumping: the design of the frog muscular system.," *Science (New York, N.Y.)*, vol. 263, pp. 370–2, Jan. 1994.

[76] Man, H. D., Lefeber, D., and Vermeulen, J., "Control on irregular terrain of a hopping robot with one articulated leg," *ICAR Workshop II: New Approaches on Dynamic ...*, 1997.

[77] Marsh, R., "Jumping ability of anurans.," pp. 51 – 111, 1994.

[78] Matsuoka, K., "A mechanical model of repetitive hopping movements," *Biomechanisms*, vol. 5, no. 2, pp. 251–258, 1980.

[79] McGeer, T., "Passive dynamic walking," *The International Journal of Robotics Research*, 1990.

[80] McGowan, C., "The mechanics of jumping versus steady hopping in yellow-footed rock wallabies," *Journal of experimental biology*, vol. 208, no. 14, pp. 2741–2751, 2005.

[81] McMahon, T. a. and Cheng, G. C., "The mechanics of running: how does stiffness couple with speed?," *Journal of biomechanics*, vol. 23 Suppl 1, pp. 65–78, Jan. 1990.

[82] McNeill Alexander, R., *Elastic mechanisms in animal movement*. Cambridge [etc.]: Cambridge University Press, 1988.

[83] Mehrandezh, M., "Jumping height control of an electrically actuated, one-legged hopping robot: modelling and simulation," *Decision and Control, 1995., Proceedings of the 34th IEEE Conference on*, 1995.

[84] Morrey, J. and Lambrecht, B., "Highly mobile and robust small quadruped robots," in *Intelligent Robots and Systems, 2003.(IROS 2003). Proceedings. 2003 IEEE/RSJ International Conference on*, 2003.

[85] Niiyama, R. and Kuniyoshi, Y., "A Pneumatic Biped with an Artificial Musculoskeletal System," in *4th Int. Symposium on Adaptive Motion of Animals and Machines*, pp. 80–81, 2008.

[86] Niiyama, R., Nagakubo, A., and Kuniyoshi, Y., "Mowgli: A bipedal jumping and landing robot with an artificial musculoskeletal system," in *Robotics and Automation, 2007 IEEE International Conference on*, no. April, pp. 2546–2551, IEEE, 2007.

[87] Ohashi, E. and Ohnishi, K., "Hopping height control for hopping robots," *Electrical Engineering in Japan*, vol. 155, pp. 64–71, Apr. 2006.

[88] Okubo, O., Nakano, E., and Handa, M., "Design of a jumping machine using self-energizing spring," *Intelligent Robots and Systems' 96, IROS 96, Proceedings of the 1996 IEEE/RSJ International Conference on*, 1996.

[89] Pandy, M. G., Zajac, F. E., Sim, E., and Levine, W. S., "An optimal control model for maximum-height human jumping.," *Journal of biomechanics*, vol. 23, pp. 1185–98, Jan. 1990.

[90] Pandy, M. and Zajac, F., "Optimal muscular coordination strategies for jumping," *Journal of biomechanics*, vol. 24, no. 1, pp. 1–10, 1991.

[91] Papantoniou, K., "Electromechanical design for an electrically powered, actively balanced one leg planar robot," *Intelligent Robots and Systems' 91.'Intelligence for Mechanical Systems, Proceedings IROS'91. IEEE/RSJ International Workshop on*, 1991.

[92] Peck, M., "Dynamics of a gyroscopic hopping rover," in *Proceeding of the 11 th Annual AAS/AIAA Space Flight Mechanics Meeting, Santa Barbara, CA*, 2001.

[93] Pfeifer, R., Lungarella, M., and Iida, F., "Self-organization, embodiment, and biologically inspired robotics.," *Science (New York, N.Y.)*, vol. 318, pp. 1088–93, Nov. 2007.

[94] Playter, R., Buehler, M., and Raibert, M., "Bigdog, unmanned systems technology viii," in *Proc. SPIE*, vol. 6230, 2006.

[95] Prosser, J. and Kam, M., "Vertical control for a mechanical model of the one-legged hopping machine," in *Control Applications, 1992., First IEEE Conference on*, 1992.

[96] Raibert, M., "Running on four legs as though they were one," *Robotics and Automation, IEEE Journal of*, vol. 2, no. 2, pp. 70–82, 1986.

[97] Raibert, M., *Legged robots that balance*. The MIT Press, Cambridge, MA, 1985.

[98] Raibert, M. and Brown Jr., H., "Experiments in balance with a 2D one-legged hopping machine," *Journal of Dynamic Systems, Measurement, and Control*, vol. 106, pp. 75–81, 1984.

[99] Rand, A., "Jumping ability of certain anurans, with notes on endurance," *Copeia*, vol. 1952, no. 1, pp. 15–20, 1952.

[100] Rand, A. and Rand, P., "The relation of size and distance jumped in Bufo marinus," *Herpetologica*, vol. 22, no. 3, pp. 206–209, 1966.

[101] Ringrose, R., "Self-stabilizing running," in *Robotics and Automation, 1997. Proceedings., 1997 IEEE International Conference on*, 1997.

[102] Roberts, T. and Marsh, R., "Probing the limits to muscle-powered accelerations: lessons from jumping bullfrogs," *Journal of Experimental Biology*, vol. 206, no. 15, pp. 2567—-2580, 2003.

[103] Sato, A., *A Planar Hopping Robot with One Actuator*. PhD thesis, 2004.

[104] Sayyad, A., Seth, B., and Seshu, P., "Single-legged hopping robotics researchA review," *Robotica*, vol. 25, pp. 1–27, Apr. 2007.

[105] Scarfogliero, U., Stefanini, C., and Dario, P., "Design and Development of the Long-Jumping Grillo Mini Robot," in *2007 IEEE ICRA*, no. April, (Rome, Italy), pp. 10–14, 2007.

[106] Seyfarth, A., Blickhan, R., and Van Leeuwen, J., "Optimum take-off techniques and muscle design for long jump," *Journal of Experimental Biology*, vol. 203, no. 4, pp. 741–750, 2000.

[107] Stoeter, S. and Rybski, P., "Autonomous stair-hopping with scout robots," in *Intelligent Robots and Systems, 2002. IEEE/RSJ International Conference on*, 2002.

[108] Takeuchi, K. and Kuswadi, S., "Continuous hopping motion control experiment of one linear actuator robot," in *SICE 2002. Proceedings of the 41st SICE Annual Conference*, 2002.

[109] Treff, H., "Der Absprungwinkel beim schrägen Sprung des Galagos (Galago senegalensis)," *Journal of Comparative Physiology A: Neuroethology, Sensory, Neural, and Behavioral Physiology*, vol. 132, 1970.

[110] Tsukagoshi, H. and Sasaki, M., "Design of a higher jumping rescue robot with the optimized pneumatic drive," in *Robotics and Automation, 2005. ICRA 2005. Proceedings of the 2005 IEEE International Conference on*, no. April, pp. 1276–1283, 2005.

[111] Uno, K., Ohmori, M., and Kondo, R., "A hopping robot with impulsive actuator," in *SICE 2002. Proceedings of the 41st SICE Annual Conference*, 2002.

[112] van Soest, A., Schwab, A., Bobbert, M., and van Ingen Schenau, G., "The influence of the biarticularity of the gastrocnemius muscle on vertical-jumping achievement," *Journal of biomechanics*, vol. 26, no. 1, pp. 1–8, 1993.

[113] Vanhooydonck, B. and Aerts, P., "Power generation during locomotion in Anolis lizards: an ecomorphological approach," *Ecology and Biomechanics: A Mechanical Approach to the Ecology of Animals and Plants*, pp. 253–269, 2006.

[114] Voigt, M., Simonsen, E., Dyhre-Poulsen, P., and Klausen, K., "Mechanical and muscular factors influencing the performance in maximal vertical jumping after different prestretch loads," *Journal of biomechanics*, vol. 28, no. 3, 1995.

[115] Wei, T., Nelson, G., and Quinn, R., "Design of a 5-cm monopod hopping robot," in *Robotics and Automation, 2000. Proceedings. ICRA'00. IEEE International Conference on*, 2000.

[116] Wilson, R., Franklin, C., and James, R., "Allometric scaling relationships of jumping performance in the striped marsh frog Limnodynastes peronii," *Journal of Experimental Biology*, vol. 1946, pp. 1937–1946, 2000.

[117] Woledge, R., Curtin, N., and Homsher, E., "Energetic aspects of muscle contraction.," *Monographs of the Physiological society*, vol. 41, p. 1, 1985.

[118] Yeadon, M., "The simulation of aerial movement II. A mathematical inertia model of the human body," *Journal of Biomechanics*, 1990.

[119] Zajac, F., Zomlefer, M., and Levine, W., "Hindlimb muscular activity, kinetics and kinematics of cats jumping to their maximum achievable heights," *Journal of Experimental Biology*, vol. 94304, no. 153, pp. 73–86, 1981.

[120] Zeglin, G., *Uniroo–a one legged dynamic hopping robot.* Dissertation, Massachusetts Institute of Technology, 1991.

[121] Zhang, W. and Wang, G., "Toward a folding-legged uniped that can learn to jump," in *Systems, Man, and Cybernetics, 1997. Computational Cybernetics and Simulation., 1997 IEEE International Conference on*, 1997.

[122] Zug, G., "Anuran locomotion: structure and function. I. Preliminary observations on relation between jumping and osteometrics of appendicular and postaxial skeleton," *Copeia*, 1972.

[123] Zug, G., "Anuran locomotion-structure and function, II: Jumping performance of semiaquatic, terrestrial, and arboreal frogs.," *Smithsonian Contributions to Zoology*, no. 276, 1978.